Earth as a transducer for dark-photon and ALP dark-matter detection

IDM 2022
14th International Conference on Identification of Dark Matter

July 21, 2022

Vienna, Austria

M.A.F., P. W. Graham, S. Kalia, D. F. Jackson Kimball. Phys. Rev. D **104**, 075023 (2021) [arXiv:2106.00022].
M.A.F., P. W. Graham, S. Kalia, D. F. Jackson Kimball. Phys. Rev. D **104**, 095032 (2021) [arXiv:2108.08852].
A. Arza, M.A.F., P. W. Graham, S. Kalia, D. F. Jackson Kimball. Phys. Rev. D **105**, 095007 (2022) [arXiv:2112.09620].
… and forthcoming work

Michael A. Fedderke

mfedderke@jhu.edu
mfedderke.com

JOHNS HOPKINS UNIVERSITY

Two takeaways

New magnetic-field signal of ultralight DPDM and ALPs

New direct constraints from a signal search in an existing dataset

Ultralight Bosonic Dark Matter

- This talk: $m_{\rm DM} \sim 10^{-17}$eV within a factor of a few $\quad (f_{\rm DM} \sim$ mHz$)$
- Classical field description

$$\phi(\mathbf{x}, t) \sim \frac{\sqrt{\rho_{\rm DM}}}{m_{\rm DM}} \cos(\omega_{\rm DM} t - \mathbf{k}_{\rm DM} \cdot \mathbf{x} + \alpha) \sim \frac{\sqrt{\rho_{\rm DM}}}{m_{\rm DM}} \cos(m_{\rm DM} t + \alpha')$$

  - $\tau_{\rm coh} \sim 10^6\, T_{\rm osc}$
  - $\lambda_{\rm coh} \sim 10^3\, \lambda_{\rm Compton}$

- Two selected candidates: JCAP 06 (2012) 013 [arXiv:1201.5902]
  - Kinetically Mixed Dark Photons (DPDM)

$$\mathscr{L} = \mathscr{L}_{\rm SM} - \frac{1}{4}(F')^2 + \frac{1}{2} m_{A'}^2 (A')^2 + \frac{\epsilon}{2} F F' \qquad (\epsilon \ll 1)$$

Phys. Lett. B 166 (1986) 196–198;
Phys. Rev. D 84 (2011) 103501 [arXiv:1105.2812]

  - Axion-like Particles (ALPs)

Phys. Rev. Lett. 38 (1977) 1440–1443; Phys. Rev. Lett. 40 (1978) 223–226; Phys. Rev. Lett. 40 (1978) 279–282.
JHEP 06 (2006) 051 [arXiv:hep-th/0605206]; Phys. Rev. D 81 (2010) 123530 [arXiv:0905.4720]

$$\mathscr{L} = \mathscr{L}_{\rm SM} + \frac{1}{2}(\partial_\mu \phi)^2 - \frac{1}{2} m_\phi^2 \phi^2 + \frac{1}{4} g_{\phi\gamma} \phi F \tilde{F}$$

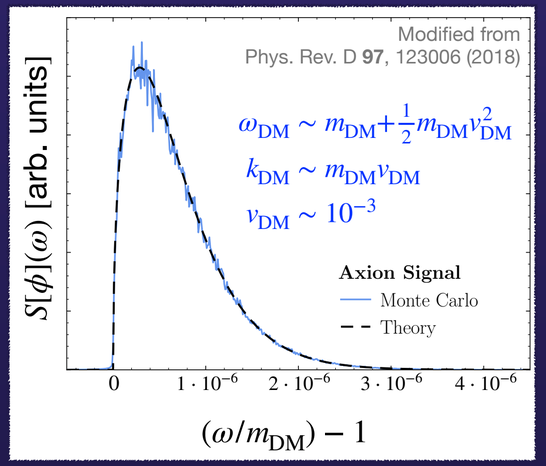

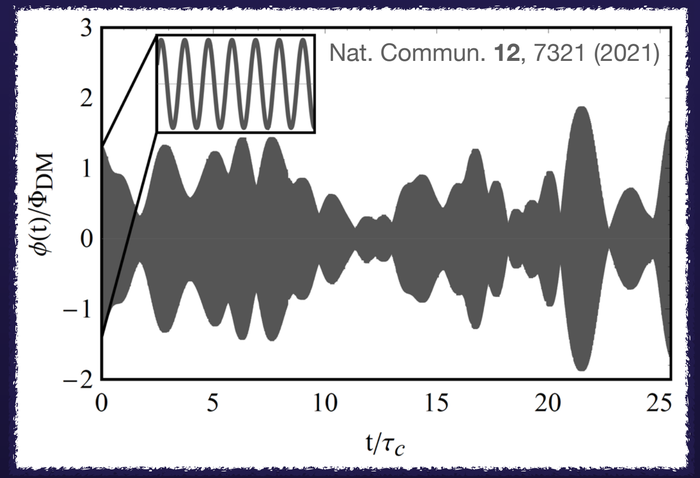

Note: ϵ is dimensionless, $g_{\phi\gamma}$ has dimensions of $(\text{mass})^{-1}$

Couplings to the EM sector

$$\mathscr{L} \supset \frac{\epsilon}{2} F F'$$

$$\mathscr{L} \supset \frac{g_{\phi\gamma}}{4} \phi F \tilde{F}$$

Mixings with the Standard Model electromagnetic sector

cause **observable EM effects**

that **inherent DM properties**:

- oscillatory with period set by m_{DM}
- phase-coherent over long times
- phase-coherent over large distances

Such as…

Reminder of some DPDM pheno

Phys. Rev. D **92** (2015) 075012 [arXiv: 1411.7382]
IEEE Trans. Appl. Supercond. 27 (2017) 4, 1400204 [arXiv:1610.09344],
Springer Proc. Phys. 245 (2020) 139-145 [arXiv:1906.08814]

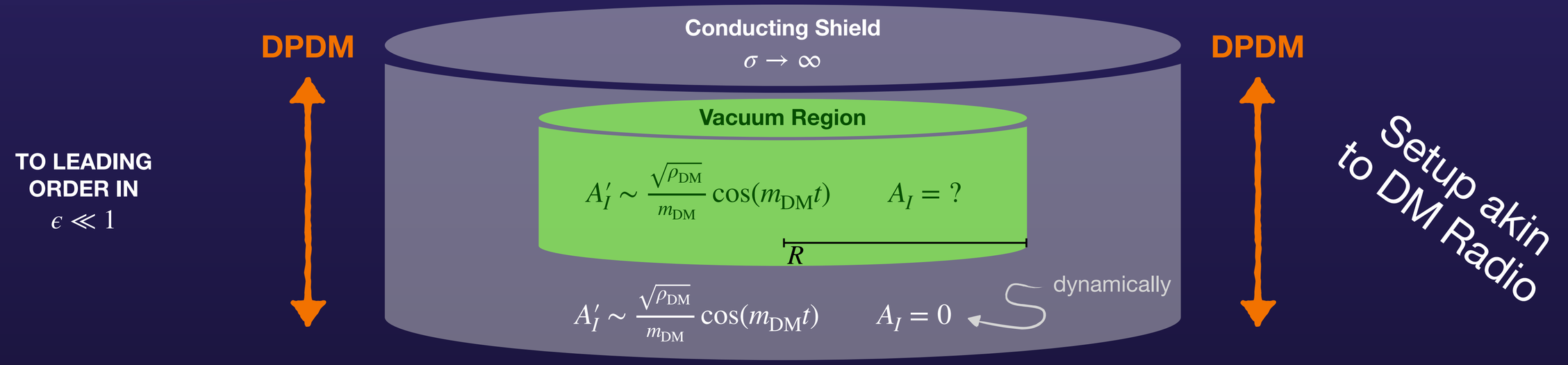

- Observable magnetic field generated in the shielded vacuum region

$$B_\phi(r \sim R) \sim R J_{\rm eff} \sim \varepsilon m_{A'} R \sqrt{\rho_{\rm DM}} \cos(m_{\rm DM} t)$$

- Suppressed by a ratio of length scales $\sim m_{A'} R \sim R/\lambda_{\rm Compton}$.

Michael A. Fedderke (JHU)

“You’re gonna need a bigger boat”

- Effects decouple as DPDM mass drops below the inverse size of the box.
- What if we want to look for DPDM with $m_{A'} \lesssim 1/(\text{size of lab}) \sim 10^{-7}\,\text{eV}$?

“You’re gonna need a bigger boat”

- Effects decouple as DPDM mass drops below the inverse size of the box.
- What if we want to look for DPDM with $m_{A'} \lesssim 1/(\text{size of lab}) \sim 10^{-7}\,\text{eV}$?
- **Our work picks up here: look for large natural objects that act like EM shields!**

“You’re gonna need a bigger boat”

- Effects decouple as DPDM mass drops below the inverse size of the box.
- What if we want to look for DPDM with $m_{A'} \lesssim 1/(\text{size of lab}) \sim 10^{-7}\,\text{eV}$?
- **Our work picks up here:** **look for large natural objects that act like EM shields!**
- The Earth?

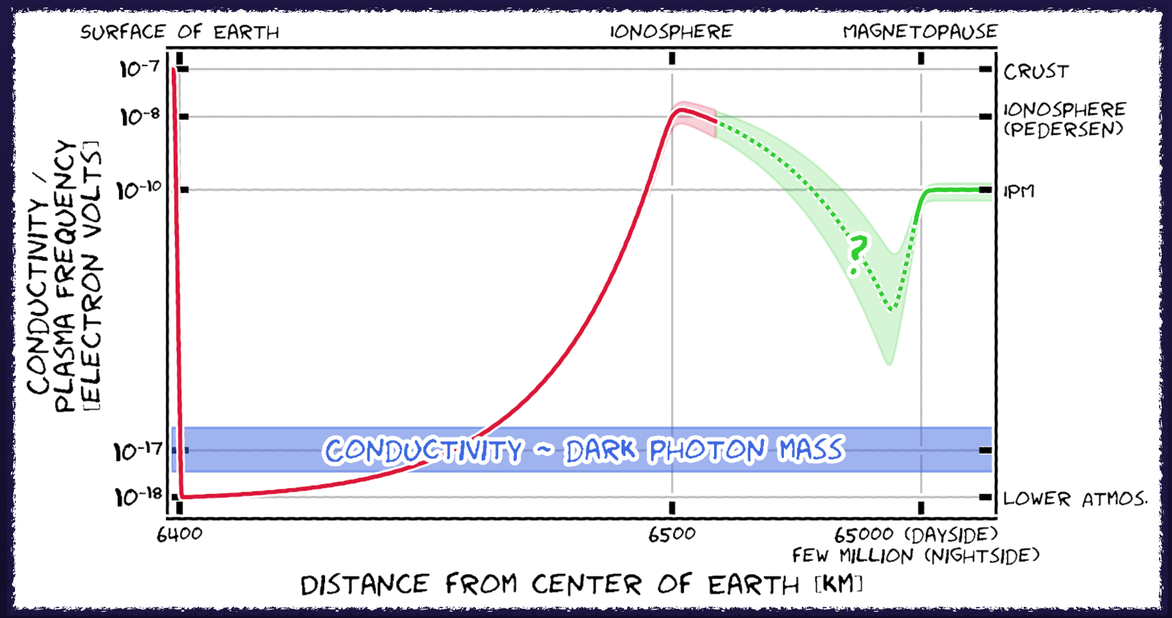

Simplified model

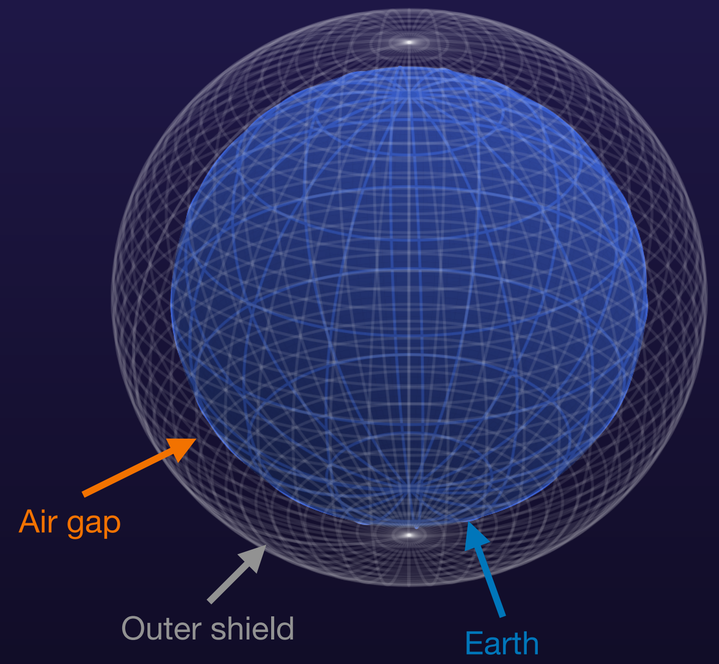

“You’re gonna need a bigger boat”

- Effects decouple as DPDM mass drops below the inverse size of the box.
- What if we want to look for DPDM with $m_{A'} \lesssim 1/(\text{size of lab}) \sim 10^{-7}\,\text{eV}$?
- **Our work picks up here:** **look for large natural objects that act like EM shields!**
- The Earth?

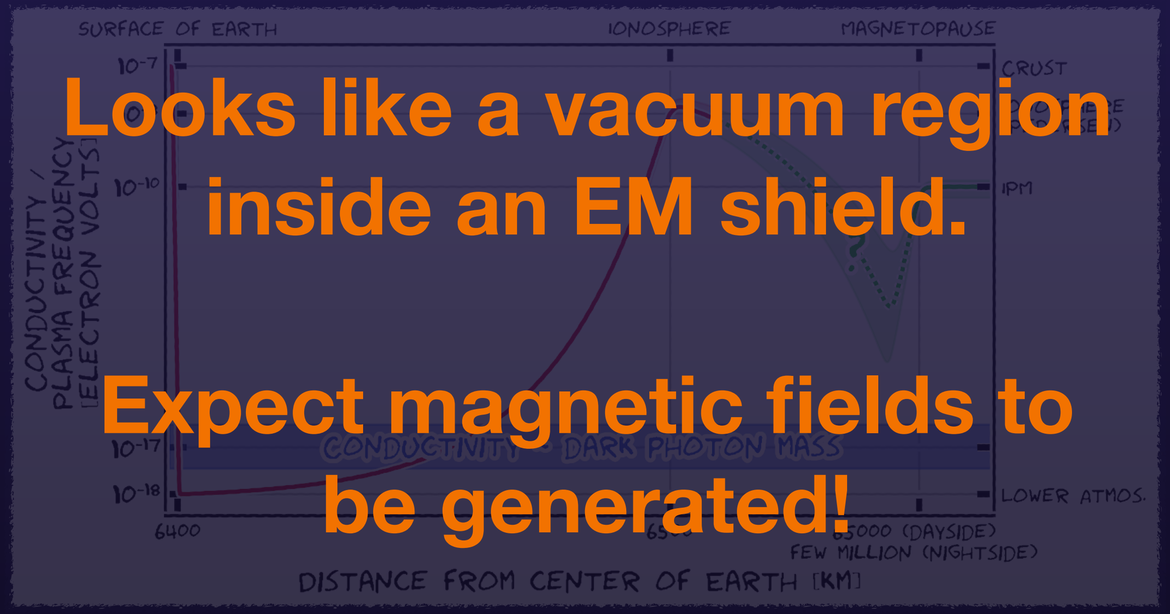

Looks like a vacuum region inside an EM shield.

Expect magnetic fields to be generated!

Simplified model

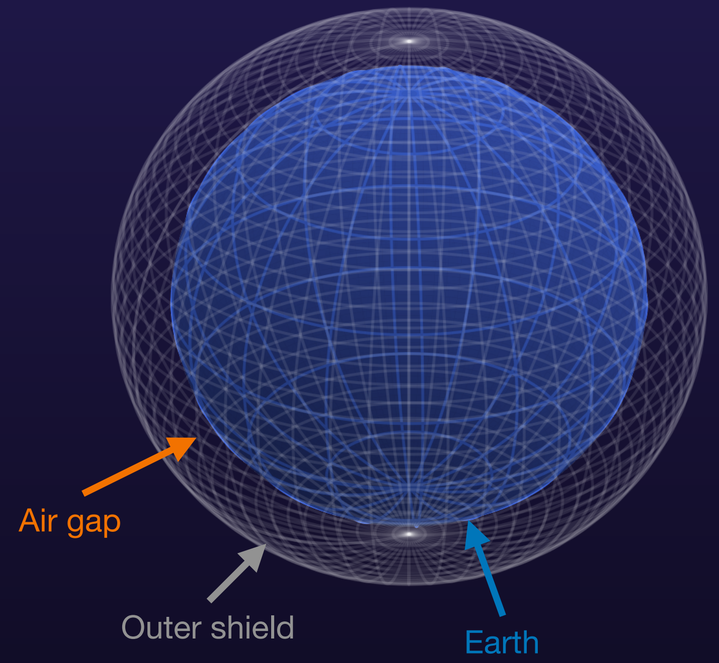

PRD **104**, 075023 (2021)
PRD **104**, 095032 (2021)

A new signal of DPDM

A TERRESTRIAL MAGNETIC FIELD AT GROUND LEVEL

Vector spherical harmonics

Location (lat/long) on surface of Earth

$$\mathbf{B}(\Omega, t) = \varepsilon m_{A'} R_\oplus \times \sqrt{\frac{\pi}{3}} m_{A'} \sum_{m=-1}^{1} A'_m \tilde{\mathbf{\Phi}}_{1m}(\Omega) e^{-i(m_{A'} - 2\pi f_d m)t} \qquad \frac{1}{2} m_{A'}^2 \langle |A'|^2 \rangle_{T \gg \tau_{\rm coh}} = \rho_{\rm DM}$$

$$|B| \sim \varepsilon m_{A'} R_\oplus \sqrt{\rho_{\rm DM}} \sim 0.7\,\text{nG} \times \left(\frac{\varepsilon}{10^{-5}}\right) \times \left(\frac{m_{A'}}{4 \times 10^{-17}\,\text{eV}}\right)$$

- **OSCILLATES**: $f = m_{A'}/(2\pi)$ (some complications that I'll ignore here)
- **NARROWBAND**: $\Delta f/f \sim v_{\rm DM}^2 \sim 10^{-6}$
- **PRESENT AND IN-PHASE OVER THE ENTIRE SURFACE OF EARTH**
- **KNOWN FIELD PATTERN AND VECTORIAL ORIENTATION**

- **Suppressed by $(m_{A'} R_\oplus)$, not $(m_{A'} h_{\rm atmos.}) \ll (m_{A'} R_\oplus)$!**
- Complications and caveats arise owing to ionosphere / IPM, but this signal remains.

$1\,\text{G} = 10^{-4}\,\text{T}$

PRD **104**, 075023 (2021)
PRD **104**, 095032 (2021)

A new signal of DPDM and Axions!

A TERRESTRIAL MAGNETIC FIELD AT GROUND LEVEL

Vector spherical harmonics

Location (lat/long) on surface of Earth

$$\mathbf{B}(\Omega, t) = \varepsilon m_{A'} R_\oplus \times \sqrt{\frac{\pi}{3}} m_{A'} \sum_{m=-1}^{1} A'_m \tilde{\mathbf{\Phi}}_{1m}(\Omega) e^{-i(m_{A'} - 2\pi f_d m)t} \qquad \frac{1}{2} m_{A'}^2 \langle |A'|^2 \rangle_{T \gg \tau_{\rm coh}} = \rho_{\rm DM}$$

$$|B| \sim \varepsilon m_{A'} R_\oplus \sqrt{\rho_{\rm DM}} \sim 0.7\,\text{nG} \times \left(\frac{\varepsilon}{10^{-5}}\right) \times \left(\frac{m_{A'}}{4 \times 10^{-17}\,\text{eV}}\right)$$

- **OSCILLATES**: $f = m_{A'}/(2\pi)$ (some complications that I'll ignore here)
- **NARROWBAND**: $\Delta f/f \sim v_{\rm DM}^2 \sim 10^{-6}$
- **PRESENT AND IN-PHASE OVER THE ENTIRE SURFACE OF EARTH**
- **KNOWN FIELD PATTERN AND VECTORIAL ORIENTATION**

- **Suppressed by $(m_{A'} R_\oplus)$, not $(m_{A'} h_{\rm atmos.}) \ll (m_{A'} R_\oplus)$!**
- Complications and caveats arise owing to ionosphere / IPM, but this signal remains.

Michael A. Fedderke (JHU)

$1\,\text{G} = 10^{-4}\,\text{T}$

PRD **104**, 075023 (2021)
PRD **104**, 095032 (2021)

A new signal of DPDM and Axions!

A TERRESTRIAL MAGNETIC FIELD AT GROUND LEVEL

Vector spherical harmonics

Location (lat/long) on surface of Earth

$$\mathbf{B}(\Omega, t) = \varepsilon m_{A'} R_\oplus \times \sqrt{\frac{\pi}{3}} m_{A'} \sum_{m=-1}^{1} A'_m \tilde{\mathbf{\Phi}}_{1m}(\Omega) e^{-i(m_{A'} - 2\pi f_d m)t} \qquad \frac{1}{2} m_{A'}^2 \langle |A'|^2 \rangle_{T \gg \tau_{\rm coh}} = \rho_{\rm DM}$$

$$|B| \sim \varepsilon m_{A'} R_\oplus \sqrt{\rho_{\rm DM}} \sim 0.7\,\text{nG} \times \left(\frac{\varepsilon}{10^{-5}}\right) \times \left(\frac{m_{A'}}{4 \times 10^{-17}\,\text{eV}}\right)$$

$$\mathscr{L} \supset g_{\phi\gamma} \phi \mathbf{E} \cdot \mathbf{B}_\oplus$$

- **OSCILLATES**: $f = m_{A'}/(2\pi)$ (some complications that I'll ignore here)
- **NARROWBAND**: $\Delta f/f \sim v_{\rm DM}^2 \sim 10^{-6}$
- **PRESENT AND IN-PHASE OVER THE ENTIRE SURFACE OF EARTH**
- **KNOWN FIELD PATTERN AND VECTORIAL ORIENTATION**

Rough translation

$$\varepsilon m_{A'} \leftrightarrow g_{\phi\gamma} B_\oplus$$

Assuming DM field-amplitude normalisations

Different detailed field pattern

$$|B| \sim 1\,\text{nG} \times \left(\frac{g_{\phi\gamma}}{10^{-10}\,\text{GeV}^{-1}}\right)$$

- **Suppressed by $(m_{A'} R_\oplus)$, not $(m_{A'} h_{\rm atmos.}) \ll (m_{A'} R_\oplus)$!**
- Complications and caveats arise owing to ionosphere / IPM, but this signal remains.

$1\,\text{G} = 10^{-4}\,\text{T}$

SuperMAG

https://supermag.jhuapl.edu
Eos **90** (2009) 230-231
J. Geophys. Res. Space Phys. **117** (2012) A09213

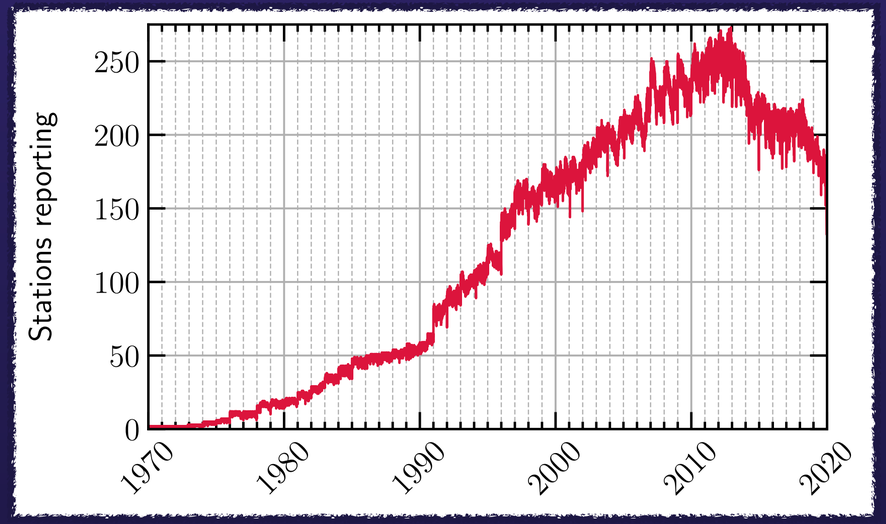

- Geophysics to the rescue!
- Collaboration based at JHU-APL (J. W. Gjerloev, PI).
  Many contributors. See acknowledgments slide at end of talk
- Make publicly available a database of:
  - Unshielded magnetic field measurements
  - at $\mathcal{O}(500)$ magnetometer stations; maximally, $\mathcal{O}(250)$ reporting at any single time
  - widely geographically distributed over the Earth's surface
  - in time-series
  - with 60s resolution*
  - since ~1970 (more data at later times)
- **Near-ideal dataset to analyse for our new signals**

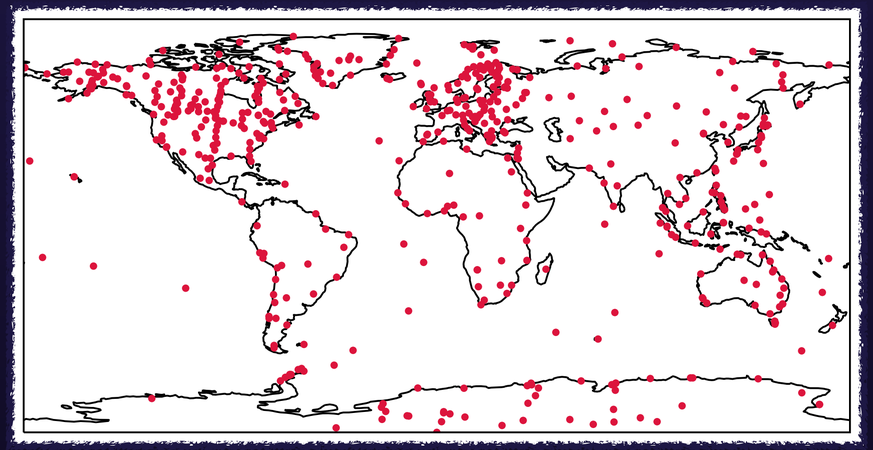

*a smaller dataset with 1s resolution is also available… see later in the talk

PRD **104**, 075023 (2021)
PRD **104**, 095032 (2021)

DPDM Results

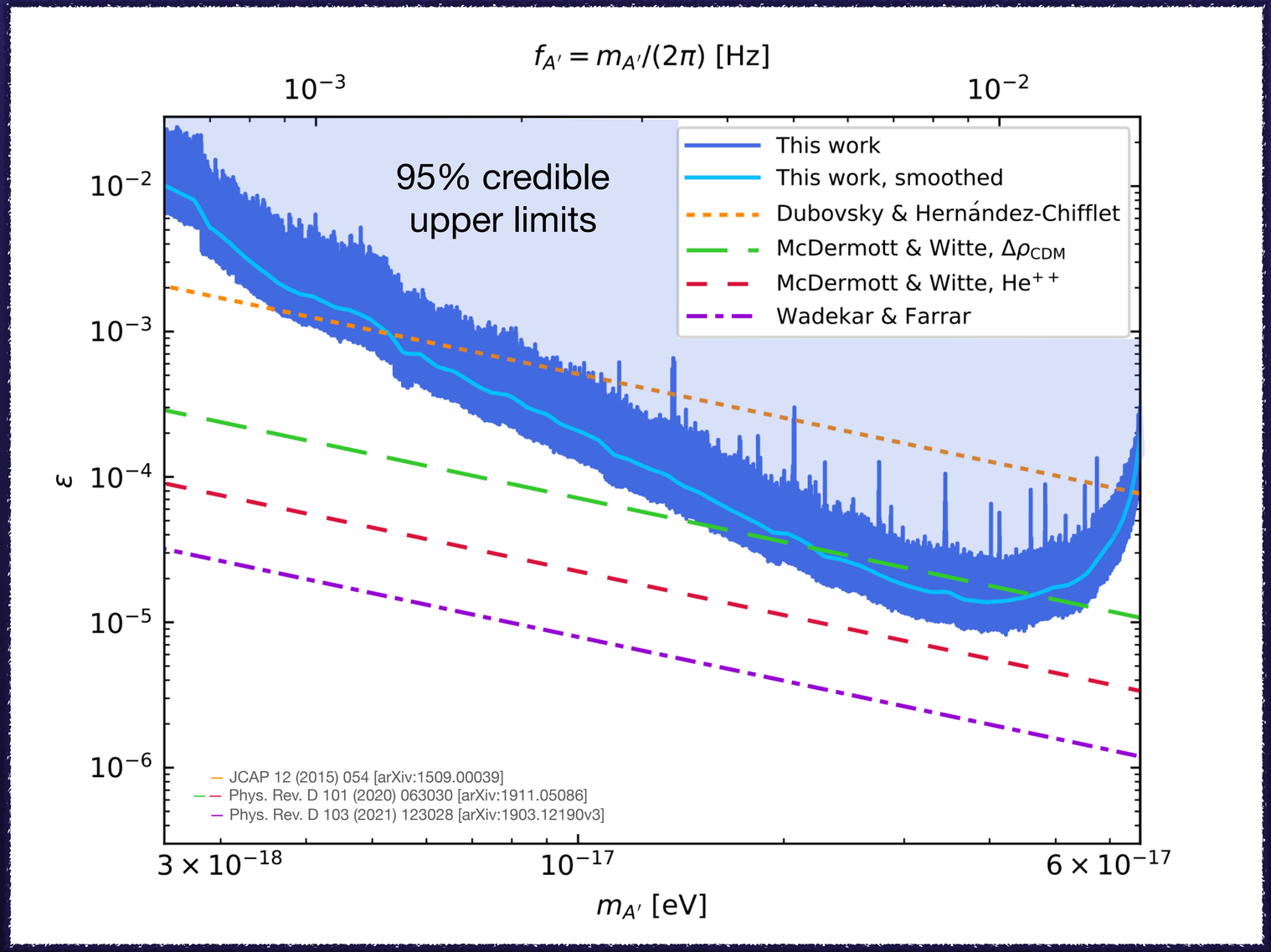

- 30 naive signal candidates (spikes) identified
- Reject 24 completely via r**obustness tests**
- 6 remaining candidates in strong tension with robustness tests, or have other issues
- **We do <u>not</u> claim any robust evidence for a DPDM signal**
- New limits complementary to astrophysical bounds
- Very different systematics!
- First “direct” constraints on this piece of parameter space.

PRD **104**, 075023 (2021)
PRD **104**, 095032 (2021)

DPDM Results

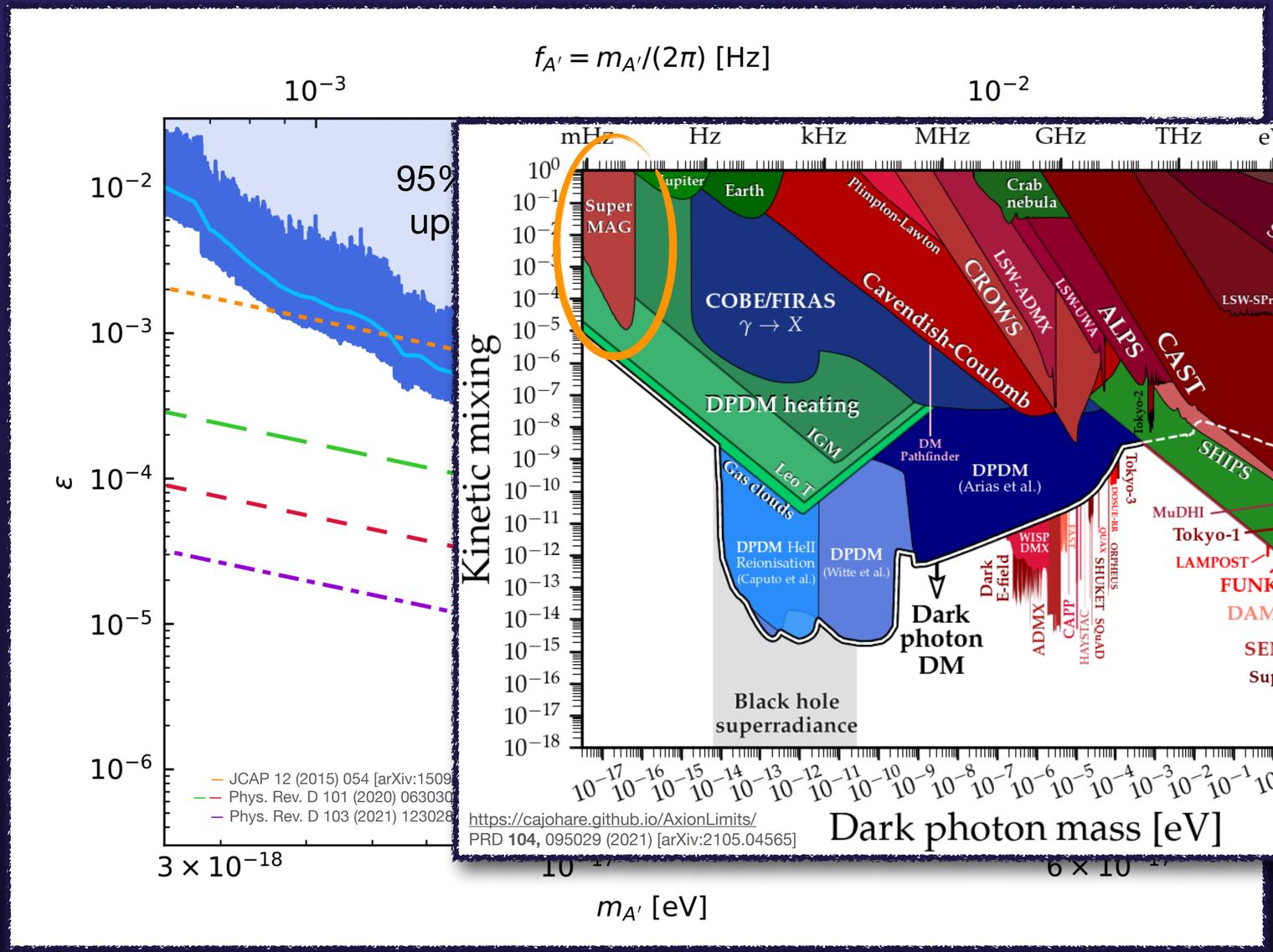

- 30 naive signal candidates (spikes) identified
- 24 completely via **ness tests**
- ning candidates in strong with robustness tests, or er issues
- **not claim any robust ce for a DPDM signal**
- its complementary to ysical bounds
- ferent systematics!
- First "direct" constraints on this piece of parameter space.

PRD **105**, 095007 (2022)

Axion Results

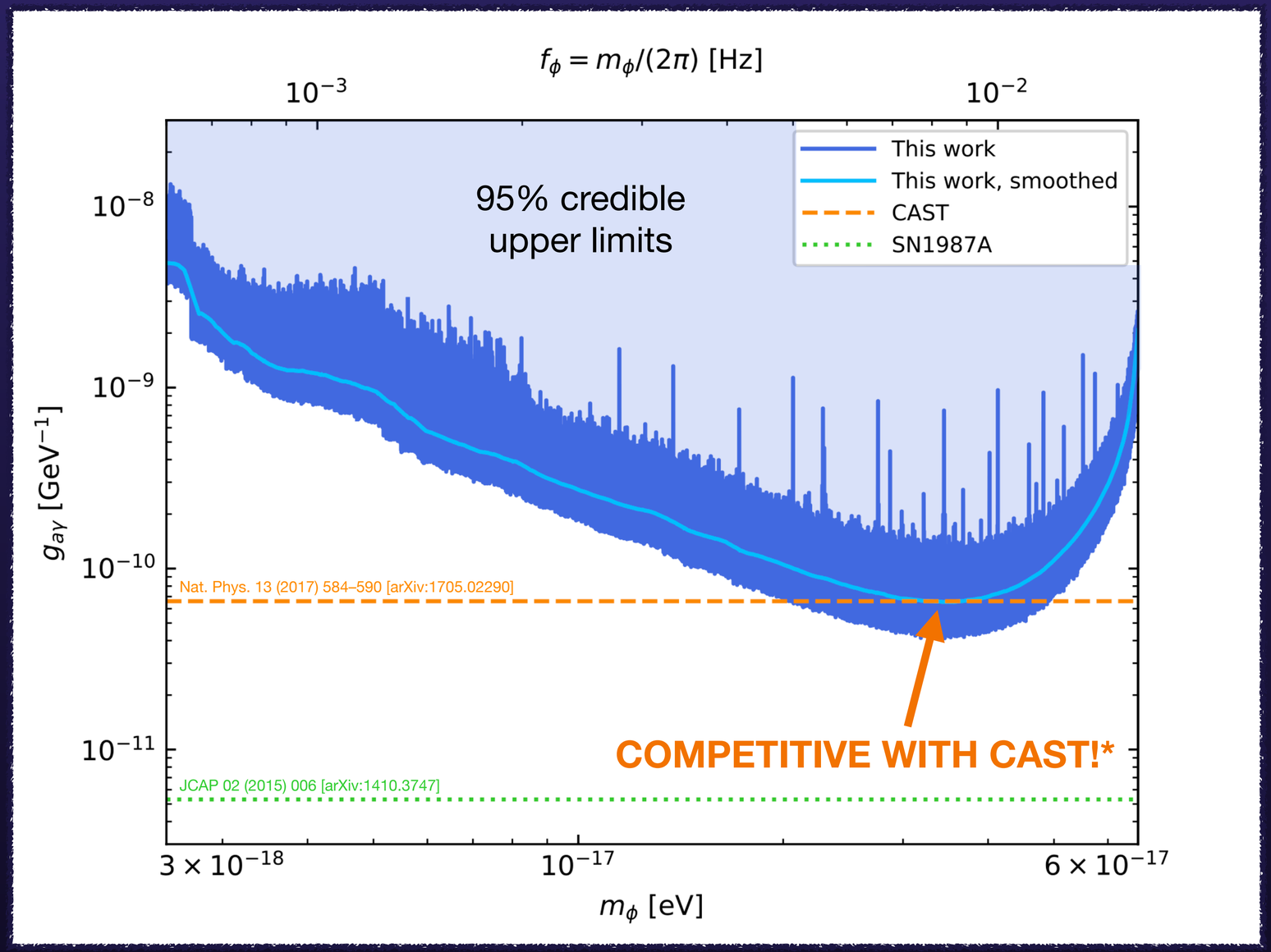

- Analysis proceed similarly, but simpler.
- Similar naive signal candidates exist (27).
- Again reject most (23) outright with robustness checks.
- Some weak signals remain (4), but have tensions with checks.
- **We do <u>not</u> claim any robust evidence for an axion signal**

*CAST does not need to assume the axion is all of the dark matter

Outlook and Future Directions

- SuperMAG has 1s resolution data available. But less of it.
- Limit of our 60s-cadence analysis at high frequencies is the measurement sampling frequency.
- In 60s data, noise appears to be falling with increasing frequency.
- Potential to **sacrifice some sensitivity*** with data quantity, but **push to higher frequency**.

*In fact, we might not even lose sensitivity. Less total time duration at 1s, but more data per time.

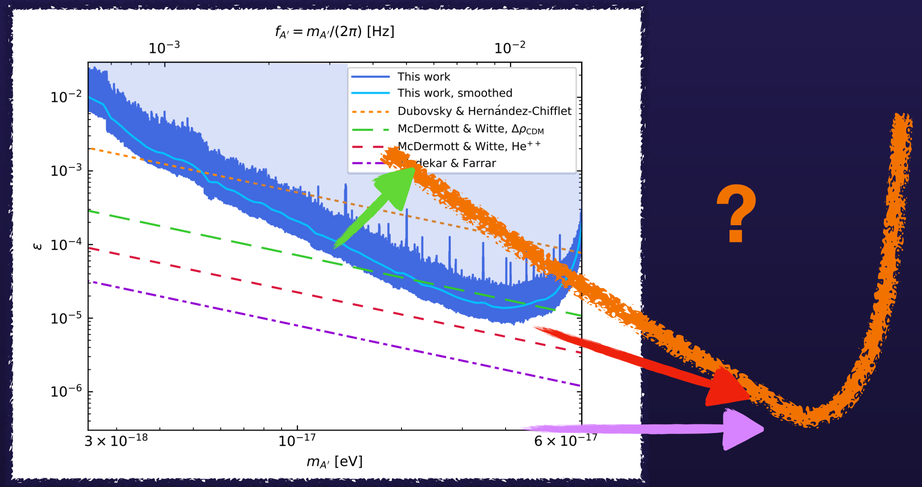

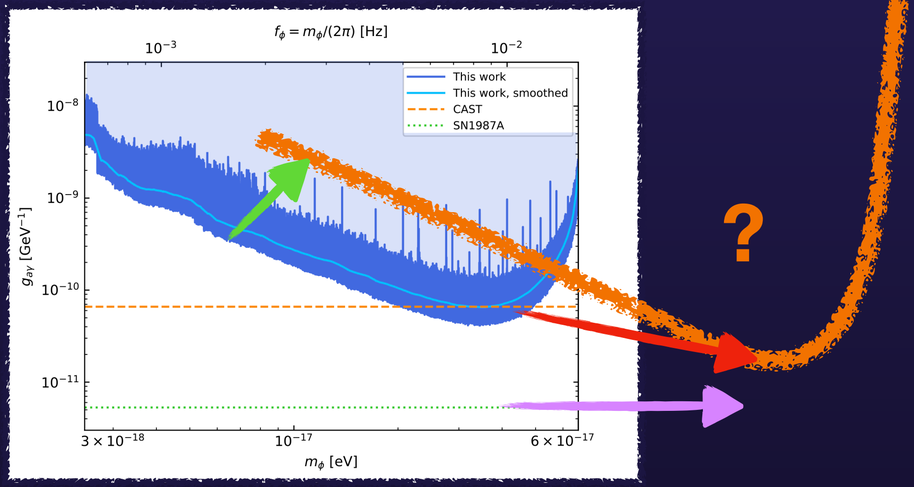

- **Win in a relative sense?** More competitive with astro limits? CAST?
- **Watch this space. Analysis in progress** (in formal collaboration with SuperMAG).
- Even higher frequencies? A dedicated network of higher-frequency magnetometers: SNIPE Hunt

There was a poster about this at the APS DAMOP Meeting in June

Summary

- Earth acts as a transducer to convert dark matter oscillations to observable EM fields
- **New signals of dark-photon and axion dark matter**
- Narrowband oscillating magnetic fields that have particular vectorial spatial pattern over whole surface of the Earth
- Ideal to search for using distributed networks of unshielded magnetometers
- Results from search in SuperMAG magnetic-field data return **no robust candidates of either DM type**
- Set limits complementary to astrophysical limits on DPDM
- Set limits beginning to be competitive with CAST for axion dark matter (at some masses)
- Higher time-resolution search underway: could extend reach to new parameter space
- Possibilities exist to have a dedicate search push to even higher frequencies.

Advertisement for some unrelated new work
Searching for DM clumps using GW detectors
[2206.14832] with S. Baum and P.W. Graham

Summary

- Earth acts as a transducer to convert dark matter oscillations to observable EM fields
- **New signals of dark-photon and axion dark matter**
- Narrowband oscillating magnetic fields that have particular vectorial spatial pattern over whole surface of the Earth
- Ideal to search for using distributed networks of unshielded magnetometers
- Results from search in SuperMAG magnetic-field data return **no robust candidates of either DM type**
- Set limits complementary to astrophysical limits on DPDM
- Set limits beginning to be competitive with CAST for axion dark matter (at some masses)
- Higher time-resolution search underway: could extend reach to new parameter space
- Possibilities exist to have a dedicate search push to even higher frequencies.

THANK YOU!

Advertisement for some unrelated new work
Searching for DM clumps using GW detectors
[2206.14832] with S. Baum and P.W. Graham

SuperMAG Data Acknowledgement

GROUND MAGNETOMETER DATA INCLUDE CONTRIBUTIONS FROM:
INTERMAGNET, Alan Thomson;
CARISMA, PI Ian Mann;
CANMOS, Geomagnetism Unit of the Geological Survey of Canada;
The S-RAMP Database, PI K. Yumoto and Dr. K. Shiokawa;
The SPIDR database;
AARI, PI Oleg Troshichev;
The MACCS program, PI M. Engebretson;
GIMA;
MEASURE, UCLA IGPP and Florida Institute of Technology;
SAMBA, PI Eftyhia Zesta;
210 Chain, PI K. Yumoto;
SAMNET, PI Farideh Honary;
IMAGE, PI Liisa Juusola;
Finnish Meteorological Institute, PI Liisa Juusola;
Sodankylä Geophysical Observatory, PI Tero Raita;
UiT the Arctic University of Norway, Tromsø Geophysical Observatory, PI Magnar G. Johnsen;
GFZ German Research Centre For Geosciences, PI Jürgen Matzka;
Institute of Geophysics, Polish Academy of Sciences, PI Anne Neska and Jan Reda;
Polar Geophysical Institute, PI Alexander Yahnin and Yarolav Sakharov;
Geological Survey of Sweden, PI Gerhard Schwarz;
Swedish Institute of Space Physics, PI Masatoshi Yamauchi;
AUTUMN, PI Martin Connors;
DTU Space, Thom Edwards and PI Anna Willer;
South Pole and McMurdo Magnetometer, PI's Louis J. Lanzarotti and Alan T. Weatherwax;
ICESTAR;
RAPIDMAG;
British Artarctic Survey;
McMac, PI Dr. Peter Chi;
BGS, PI Dr. Susan Macmillan;
Pushkov Institute of Terrestrial Magnetism, Ionosphere and Radio Wave Propagation (IZMIRAN);
MFGI, PI B. Heilig;
Institute of Geophysics, Polish Academy of Sciences, PI Anne Neska and Jan Reda;
University of L'Aquila, PI M. Vellante;
BCMT, V. Lesur and A. Chambodut;
Data obtained in cooperation with Geoscience Australia, PI Andrew Lewis;
AALPIP, co-PIs Bob Clauer and Michael Hartinger;
MagStar, PI Jennifer Gannon;
SuperMAG, PI Jesper W. Gjerloev;
Data obtained in cooperation with the Australian Bureau of Meteorology, PI Richard Marshall.

https://supermag.jhuapl.edu
Eos **90** (2009) 230-231
J. Geophys. Res. Space Phys. **117** (2012) A09213

BACKUP

Basis relationships

Kinetically Mixed Basis

$$\mathcal{L} \supset -\frac{1}{4}(F_{\rm K})_{\mu\nu}(F_{\rm K})^{\mu\nu} - \frac{1}{4}(F'_{\rm K})_{\mu\nu}(F'_{\rm K})^{\mu\nu} + \frac{\varepsilon}{2}(F_{\rm K})_{\mu\nu}(F'_{\rm K})^{\mu\nu} + \frac{1}{2}m^2_{A'}(A'_{\rm K})_\mu(A'_{\rm K})^\mu - J^\mu_{\rm EM}(A_{\rm K})_\mu,$$

Non-unitary

$$\begin{pmatrix} A_{\rm M} \\ A'_{\rm M} \end{pmatrix} = \begin{pmatrix} 1 & -\varepsilon \\ 0 & \sqrt{1-\varepsilon^2} \end{pmatrix} \begin{pmatrix} A_{\rm K} \\ A'_{\rm K} \end{pmatrix}$$

$$\begin{pmatrix} A_{\rm I} \\ A'_{\rm I} \end{pmatrix} = \begin{pmatrix} \sqrt{1-\varepsilon^2} & +\varepsilon \\ -\varepsilon & \sqrt{1-\varepsilon^2} \end{pmatrix} \begin{pmatrix} A_{\rm M} \\ A'_{\rm M} \end{pmatrix}$$

Unitary

Non-unitary

$$\begin{pmatrix} A_{\rm I} \\ A'_{\rm I} \end{pmatrix} = \begin{pmatrix} \sqrt{1-\varepsilon^2} & 0 \\ -\varepsilon & 1 \end{pmatrix} \begin{pmatrix} A_{\rm K} \\ A'_{\rm K} \end{pmatrix}$$

$$\mathcal{L} \supset -\frac{1}{4}(F_{\rm M})_{\mu\nu}(F_{\rm M})^{\mu\nu} - \frac{1}{4}(F'_{\rm M})_{\mu\nu}(F'_{\rm M})^{\mu\nu} + \frac{1}{2}\frac{m^2_{A'}}{1-\varepsilon^2}(A'_{\rm M})_\mu(A'_{\rm M})^\mu - J^\mu_{\rm EM}\left[(A_{\rm M})_\mu + \frac{\varepsilon}{\sqrt{1-\varepsilon^2}}(A'_{\rm M})_\mu\right].$$

Vacuum Mass Basis

$$\mathcal{L} \supset -\frac{1}{4}(F_{\rm I})_{\mu\nu}(F_{\rm I})^{\mu\nu} - \frac{1}{4}(F'_{\rm I})_{\mu\nu}(F'_{\rm I})^{\mu\nu} + \frac{1}{2}m^2_{A'}\left[(A'_{\rm I})_\mu(A'_{\rm I})^\mu + \frac{2\varepsilon}{\sqrt{1-\varepsilon^2}}(A_{\rm I})^\mu(A'_{\rm I})_\mu + \frac{\varepsilon^2}{1-\varepsilon^2}(A_{\rm I})_\mu(A_{\rm I})^\mu\right] - \frac{1}{\sqrt{1-\varepsilon^2}}J^\mu_{\rm EM}(A_{\rm I})_\mu.$$

Interaction Basis

DPDM Pheno I

Setup akin to DM Radio
[Phys. Rev. D **92** (2015) 075012 [arXiv: 1411.7382] IEEE Trans. Appl. Supercond. 27 (2017) 4, 1400204 [arXiv:1610.09344], Springer Proc. Phys. 245 (2020) 139-145 [arXiv:1906.08814]

- Focus on $\mathscr{L} = \mathscr{L}_{\rm SM} - \frac{1}{4}(F')^2 + \frac{1}{2}m_{A'}^2(A')^2 + \frac{\epsilon}{2}FF' \qquad (\epsilon \ll 1)$
- Same physics, different basis:

Interaction basis $\mathscr{L} \supset -\frac{1}{4}(F_I)^2 - \frac{1}{4}(F_I')^2 + \frac{1}{2}m_{A'}^2(A_I' + \varepsilon A_I)^2 - J_{\rm EM}A_I$

A_I couples to charges.
A_I' does not (sterile state).

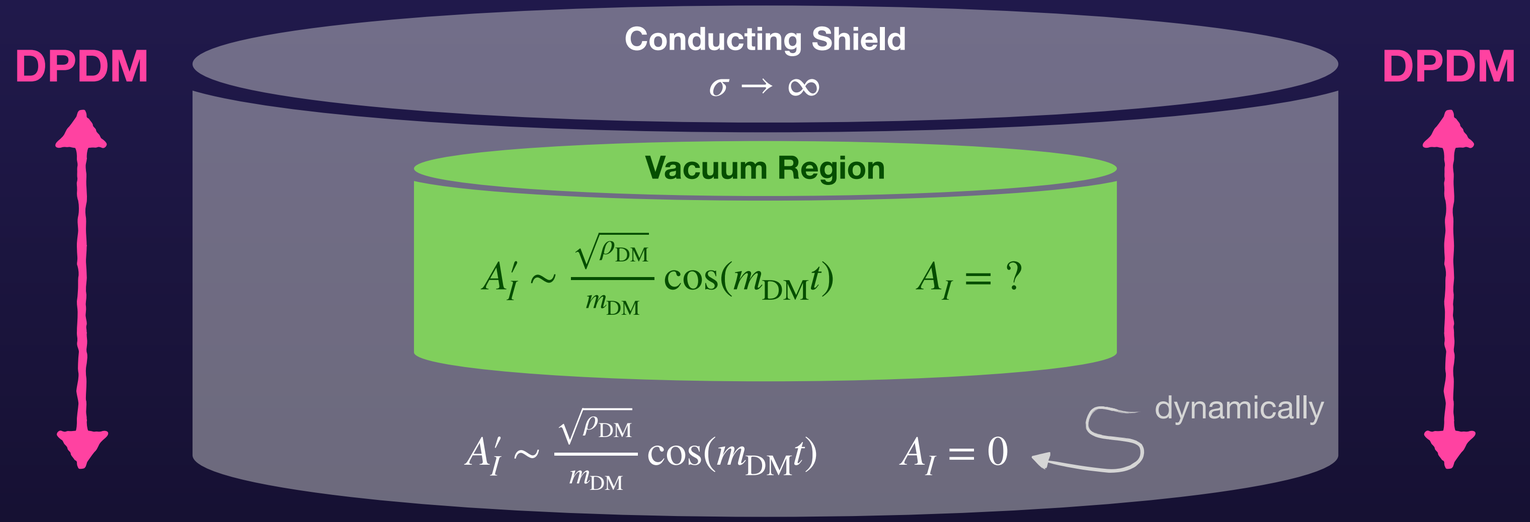

TO LEADING ORDER IN
$\epsilon \ll 1$

- Detectable field A_I in the vacuum region? Expand mass term: $\mathscr{L} \supset -(J_{\rm EM} - \varepsilon m_{A'}^2 A_I') \cdot A_I$
- **DPDM field A_I' acts as oscillating background current sourcing EM**: $J^\mu_{\rm eff} \sim -\varepsilon m_{A'}^2 (A_I')^\mu$.
- Non-relativistic limit: $\mathbf{J}_{\rm eff} \sim -\varepsilon m_{A'}^2 \mathbf{A}_I' \sim -\varepsilon m_{A'}\sqrt{\rho_{\rm DM}}\hat{\mathbf{A}}_I'$.

* or region of high plasma frequency

DPDM Pheno I

This is a two-state system: photon and dark photon

- Focus on $\mathscr{L} = \mathscr{L}_{\rm SM} - \frac{1}{4}(F')^2 + \frac{1}{2}m_{A'}^2(A')^2 + \frac{\epsilon}{2}FF' \qquad (\epsilon \ll 1)$
- This “kinetically mixed basis” of fields is not the most illuminating for qualitative understanding (or computing)
- Two other ways of writing ***the same physics*** (field re-definitions)
  - (Vacuum) Mass Basis: propagating eigenstates in vacuum

$$\mathscr{L} \supset -\frac{1}{4}(F_M)^2 - \frac{1}{4}(F'_M)^2 + \frac{1}{2}m_{A'}^2(A'_M)^2 - J_{\rm EM}(A_M + \varepsilon A'_M)$$

  - Interaction Basis: interaction eigenstates

$$\mathscr{L} \supset -\frac{1}{4}(F_I)^2 - \frac{1}{4}(F'_I)^2 + \frac{1}{2}m_{A'}^2(A'_I + \varepsilon A_I)^2 - J_{\rm EM}A_I$$

BASIS	Pro	Con
Kinetic	Easy to write down and motivate	Difficult to understand physical effects
Vacuum Mass	Vacuum propagation eigenstates	Both fields couple of SM charges
Interaction	Only one field is sourced	Fields mix under vacuum propagation

DPDM Pheno I

This is a two-state system: photon and dark photon

- Focus on $\mathscr{L} = \mathscr{L}_{\rm SM} - \frac{1}{4}(F')^2 + \frac{1}{2}m_{A'}^2(A')^2 + \frac{\epsilon}{2}FF' \qquad (\epsilon \ll 1)$
- This “kinetically mixed basis” of fields is not the most illuminating for qualitative understanding (or computing)
- Two other ways of writing ***the same physics*** (field re-definitions)
  - (Vacuum) Mass Basis: propagating eigenstates in vacuum

$$\mathscr{L} \supset -\frac{1}{4}(F_M)^2 - \frac{1}{4}(F'_M)^2 + \frac{1}{2}m_{A'}^2(A'_M)^2 - J_{\rm EM}(A_M + \varepsilon A'_M)$$

  - Interaction Basis: interaction eigenstates

$$\mathscr{L} \supset -\frac{1}{4}(F_I)^2 - \frac{1}{4}(F'_I)^2 + \frac{1}{2}m_{A'}^2(A'_I + \varepsilon A_I)^2 - J_{\rm EM}A_I$$

$$M_I = \begin{pmatrix} 0 & \varepsilon m_{A'}^2 \\ \varepsilon m_{A'}^2 & m_{A'}^2 \end{pmatrix} \quad \textbf{(vacuum)}$$

$$M_I \sim \begin{pmatrix} \Pi_{AA} & \varepsilon m_{A'}^2 \\ \varepsilon m_{A'}^2 & m_{A'}^2 \end{pmatrix} \quad \textbf{(in medium)}$$

In-medium effects can re-align the basis states

BASIS	Pro	Con
Kinetic	Easy to write down and motivate	Difficult to understand physical effects
Vacuum Mass	Vacuum propagation eigenstates	Both fields couple of SM charges
Interaction	Only one field is sourced	Fields mix under vacuum propagation
	In-medium propagation eigenstates	

The interaction basis states are approximate propagation eigenstates when:

- in a good conductor, $\sigma \gg m_{A'}^2/\omega \sim m_{A'}$
- in a region of high plasma frequency, $\omega_p \gg m_{A'}$

DPDM Pheno II

Setup akin to DM Radio
[Phys. Rev. D **92** (2015) 075012 [arXiv: 1411.7382] IEEE Trans. Appl. Supercond. 27 (2017) 4, 1400204 [arXiv:1610.09344], Springer Proc. Phys. 245 (2020) 139-145 [arXiv:1906.08814]

- Apply the Ampère-Maxwell Law to this simple geometry

$$\iint \mathbf{J} \cdot \mathbf{dA} = \oint \mathbf{B} \cdot \mathbf{dl} \Rightarrow R^2 J_{\text{eff}} \sim BR$$

Displacement current term is higher-order

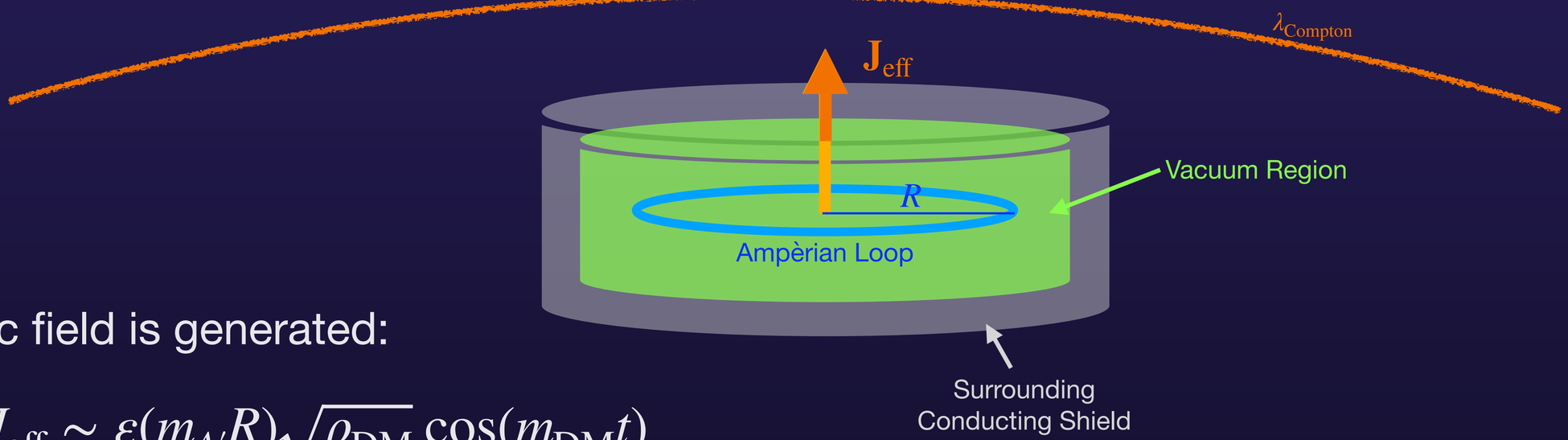

- An axial magnetic field is generated:

$$B_\phi(r \sim R) \sim RJ_{\text{eff}} \sim \varepsilon(m_{A'}R)\sqrt{\rho_{\text{DM}}}\cos(m_{\text{DM}}t)$$

- Suppressed by a ratio of length scales: $m_{A'}R \sim R/\lambda_{\text{Compton}}$.
- Electric field further suppressed by $(m_{A'}R)^2$, $v_{\text{DM}}(m_{A'}R)$

DPDM Pheno II

- Basis changes at interfaces cause interesting happen = EM signals to appear
- Consider a setup akin to DM Radio
  [Phys. Rev. D **92**, 075012, arXiv:1610.09344, arXiv:1906.08814]
- A vacuum gap in a shielded box

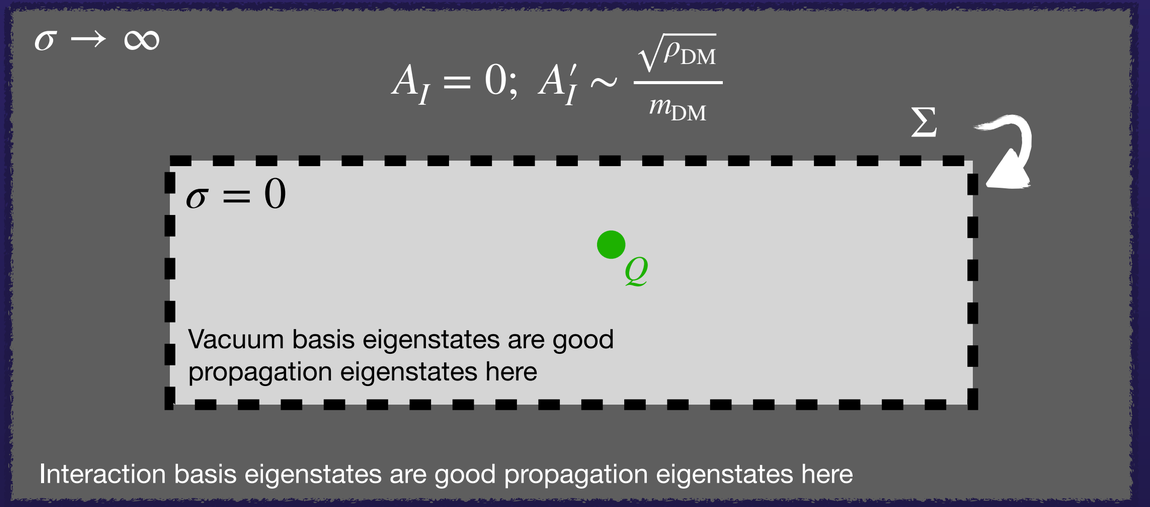

- Consider a charge Q inside the box, at $\mathbf{x}_2$. Responds to $A_I(\mathbf{x}_2) = A_M(\mathbf{x}_2) + \varepsilon A'_M(\mathbf{x}_2)$
- Need to know $A_M(\mathbf{x}_2), A'_M(\mathbf{x}_2)$! The shield sets a boundary condition:

$$A_I|_\Sigma = 0 \ \Rightarrow\ A_M|_\Sigma + \varepsilon A'_M|_\Sigma = 0; \qquad A'_I|_\Sigma \sim \frac{\sqrt{\rho_{\rm DM}}}{m_{\rm DM}} \ \Rightarrow\ A'_M|_\Sigma - \varepsilon A_M|_\Sigma \sim \frac{\sqrt{\rho_{\rm DM}}}{m_{\rm DM}}$$

$$\Rightarrow A'_M|_\Sigma \sim +\frac{\sqrt{\rho_{\rm DM}}}{m_{\rm DM}}; \qquad A_M|_\Sigma \sim -\varepsilon\frac{\sqrt{\rho_{\rm DM}}}{m_{\rm DM}}$$

- But it's vacuum inside the box: $A_M(\mathbf{x}) \sim A_M|_\Sigma \times e^{i\mathbf{k}_M\cdot\mathbf{x}}; \quad A'_M(\mathbf{x}) \sim A'_M|_\Sigma \times e^{i\mathbf{k}'_M\cdot\mathbf{x}}$
- Momenta of the vacuum eigenstates differ: $\mathbf{k}_M \neq \mathbf{k}'_M \quad\Rightarrow\quad A_M(\mathbf{x}_2) + \varepsilon A'_M(\mathbf{x}_2) \neq 0 \quad\Rightarrow\quad A_I(\mathbf{x}_2) \neq 0$

Q feels an EM force!

This is of course approximate: you actually solve the PDE

DPDM Pheno III

- What kind of force?
- Remember: $\mathscr{L} \supset \frac{1}{2} m_{A'}^2 (A_I' + \varepsilon A_I)^2 - J_{\mathrm{EM}} A_I \supset -(J_{\mathrm{EM}} - \varepsilon m_{A'}^2 A_I') \cdot A_I$
- To leading order in $\varepsilon \ll 1$, DPDM fields is an oscillating background current: $J^\mu_{\mathrm{eff}} \sim -\varepsilon m_{A'}^2 (A')^\mu$. Non-relativistic limit: $\mathbf{J}_{\mathrm{eff}} \sim -\varepsilon m_{A'}^2 \mathbf{A}'$.
- Apply the Ampère-Maxwell Law

$$\iint \mathbf{J} \cdot \mathbf{dA} = \oint \mathbf{B} \cdot \mathbf{dl} \Rightarrow R^2 J_{\mathrm{eff}} \sim BR$$

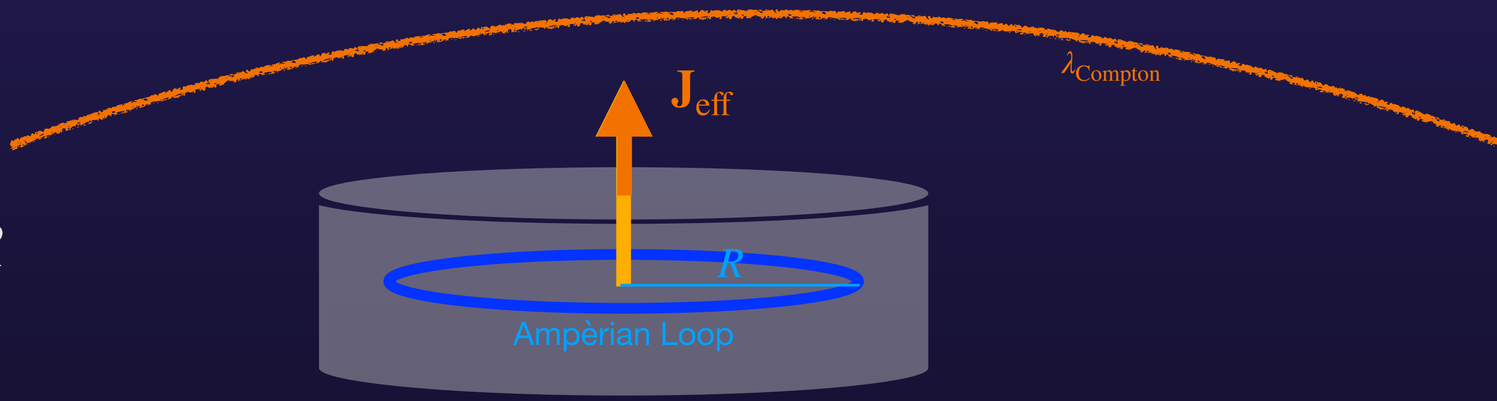

- An axial magnetic field is generated:

$$B_\phi(r \sim R) \sim R J_{\mathrm{eff}} \sim \varepsilon (m_{A'} R) \sqrt{\rho_{\mathrm{DM}}}$$

- Note: suppressed by $m_{A'} R \sim R/\lambda_{\mathrm{Compton}}$. Electric field further suppressed.

Conductivity Environment

Ground

TABLE I. Representative values for the conductivity of various parts of the bulk of the Earth. We give a description, approximate depth below Earth's surface, reference conductivity σ (or range of conductivities) in both SI and natural units,[a] active-mode skin-depth $\delta \sim (\sigma\omega/2)^{-1/2}$ (see Appendix A) for $\omega \sim \omega_\star \equiv 10^{-18}\,\mathrm{eV}$ given the reference conductivity (or range), and references for the conductivity values quoted. The specific numbers quoted here are less important than the following general conclusion: the active-mode skin-depths for the lower mantle and deeper layers are all some orders of magnitude smaller than the thicknesses of those layers, making the Earth an excellent conductor that damps the interacting component efficiently at a radius that is $\mathcal{O}(1)$ of the full radius of the Earth.

Description	Depth [km]	σ [S/m]	σ [eV]	$\delta(\omega_\star)$ [km]	Ref(s).
Surface/crust ($f \lesssim 30\,\mathrm{kHz}$)[b]	0–30	10^{-4}–10^{-2}	7×10^{-9}–7×10^{-7}	3200–320	[51]
Oceans ($f \lesssim 30\,\mathrm{kHz}$)	0–10	~ 4	$\sim 3\times10^{-4}$	~ 16	[51]
Upper mantle	30–500	$\sim 10^{-2}$	$\sim 7\times10^{-7}$	320	[52, 53]
Lower mantle (upper)	500–1000	1–10	7×10^{-4}–7×10^{-3}	30–10	[52, 53]
Lower mantle (core–mantle boundary)	~ 2900	$\sim 10^{2}$	$\sim 7\times10^{-3}$	~ 3	[54]
Outer core[c]	2900–5200	$(1.2\text{–}1.3)\times10^{6}$	~ 90–95	3.0×10^{-2}	[55]
Inner core	5200–6400	$(1.5\text{–}1.6)\times10^{6}$	$110-120$	2.5×10^{-2}	[55]

[a] Recall: $1\,\mathrm{S/m} \equiv 1/(\Omega\mathrm{m}) \approx 7.4\times10^{-5}\,\mathrm{eV} \approx 10^{11}\,\mathrm{s}^{-1}$. In older literature, units of 'e.m.u.' are sometimes used: $1\,\mathrm{S/m} = 10^{-11}\,\mathrm{e.m.u.}$
[b] Conductivity varies by geographical location (local ground composition) [51].
[c] Conductivity inferred from inner core values and comments in Ref. [55].

IPM

$$\nu = \frac{4\sqrt{2\pi}\alpha^2 n_e}{3\sqrt{m_e T_e^3}}\ln\Lambda_C \sim 10^{-20}\,\mathrm{eV}, \quad \text{Coll.}$$

$$\omega_c = \frac{eB_\odot}{m_e} \sim 6\times10^{-13}\,\mathrm{eV}, \quad \text{Cyclotron (5nT)}$$

$$\omega_p = \sqrt{\frac{4\pi n_e \alpha}{m_e}} \sim 10^{-10}\,\mathrm{eV}, \quad \text{Plasma}$$

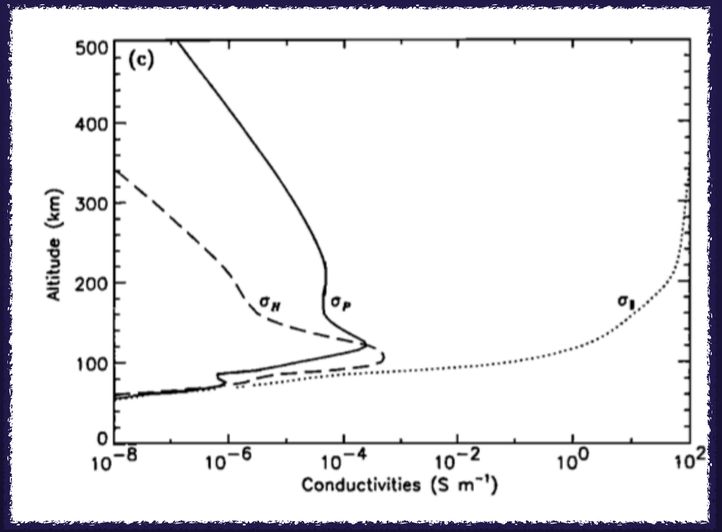

Ionosphere - parallel

$$\delta \sim \sqrt{\frac{2}{m_{A'}\sigma}} \sim 2\,\mathrm{km}\times\sqrt{\frac{10^{-18}\,\mathrm{eV}}{m_{A'}}}\times\sqrt{\frac{10^{2}\,\mathrm{S/m}}{\sigma}} \quad (6)$$

Lower Atmosphere

$$\delta \sim \sqrt{\frac{2}{m_{A'}\sigma}} \sim 1.3\,\mathrm{AU}\times\sqrt{\frac{10^{-18}\,\mathrm{eV}}{m_{A'}}}\times\sqrt{\frac{3\times10^{-14}\,\mathrm{S/m}}{\sigma}}.$$

Ionosphere - Pedersen

$$\delta \sim \sqrt{\frac{2}{m_{A'}\sigma}} \sim 1300\,\mathrm{km}\times\sqrt{\frac{10^{-18}\,\mathrm{eV}}{m_{A'}}}\times\sqrt{\frac{3\times10^{-4}\,\mathrm{S/m}}{\sigma}}. \quad (7)$$

$$\mathbf{J} = \sigma_P \mathbf{E}'_\perp + \sigma_H \mathbf{b}\times\mathbf{E}'_\perp + \sigma_\parallel E'_\parallel \mathbf{b}$$

[59] A. Richmond and J. Thayer, *Ionospheric Electrodynamics: A Tutorial*, in *Magnetospheric Current Systems (Geophysical Monograph 118)* (S. Ohtani, R. Fujii, M. Hesse and R. L. Lysak, eds.), pp. 131–146. American Geophysical Union, Washington, DC, 2000.

PRD **104**, 075023 (2021)
PRD **104**, 095032 (2021)

A new signal of DPDM I

- Spherical conductor, surrounded by a (vacuum-like) air gap, surrounded by a spherical shield (ionosphere / IPM)
- What is the field on the ground?
- Run a similar Ampèrian loop argument

$$\iint \mathbf{J}\cdot\mathbf{dA} = \oint \mathbf{B}\cdot\mathbf{dl} \Rightarrow R_\oplus^2 J_{\rm eff} \sim B R_\oplus$$

Displacement current term is higher-order

$$|B| \sim \varepsilon (m_{A'} R_\oplus)\sqrt{\rho_{\rm DM}} \sim 0.7\,{\rm nG} \times \left(\frac{\varepsilon}{10^{-5}}\right) \times \left(\frac{m_{A'}}{4\times 10^{-17}\,{\rm eV}}\right)$$

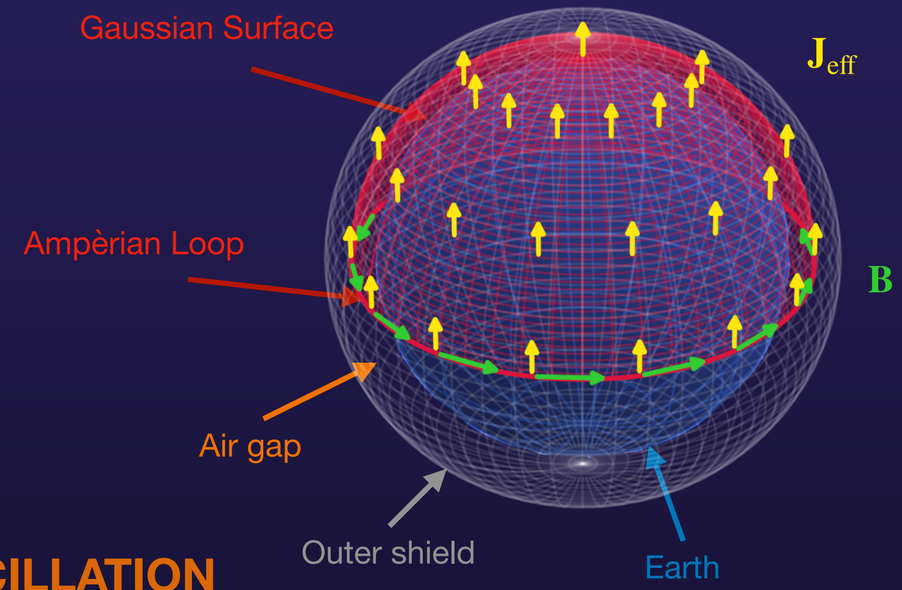

- **A PERSISTENT, GLOBAL, NARROWBAND MAGNETIC FIELD OSCILLATION WITH A KNOWN VECTORIAL PATTERN, IN-PHASE OVER THE ENTIRE SURFACE OF THE EARTH**
- The field is **very small**, but **spectral and spatial features differ from noise sources**
- **Suppressed by $(m_{A'} R_\oplus)$, not $(m_{A'} h_{\rm atmos.}) \ll (m_{A'} R_\oplus)$!**
- Complications and caveats arise owing to ionosphere / IPM, but this signal remains.

$1\,{\rm G} = 10^{-4}\,{\rm T}$

A new signal of DPDM II

PRD **104**, 075023 (2021)
PRD **104**, 095032 (2021)

- Performing the computation rigorously, we find

$$\mathbf{B}(\tilde{\Omega}, t) = \sqrt{\frac{\pi}{3}} \varepsilon m_{A'}^2 R_\oplus \sum_{m=-1}^{1} A'_m \tilde{\mathbf{\Phi}}_{1m}(\tilde{\Omega}) e^{-i(m_{A'} - 2\pi f_d m)t}$$

where $\frac{1}{2} m_{A'}^2 \langle |A'|^2 \rangle_{T \gg T_{\rm coh}} = \rho_{\rm DM}$

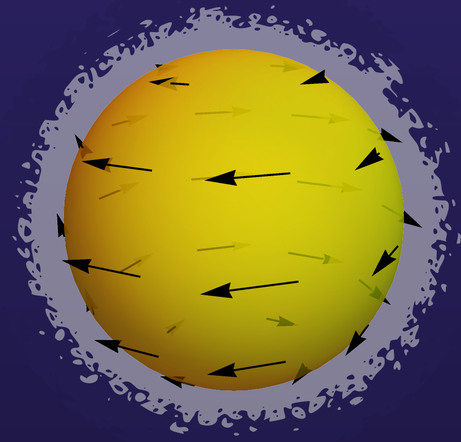

- Signal found in one type of Vector Spherical Harmonic (VSH)
- Field will be evaluated in the (rotating) Earth frame; ground magnetometer station at $\tilde{\Omega} = (\tilde{\theta}, \tilde{\phi})$
- DPDM polarization state $\mathbf{A}'$ fixed in inertial space (within coherence time / patch)
- Non-trivial frequency structure
  Sensitive to DPDM polarization state

Sidebands offset by
$f_d = 1/(\text{siderial day})$

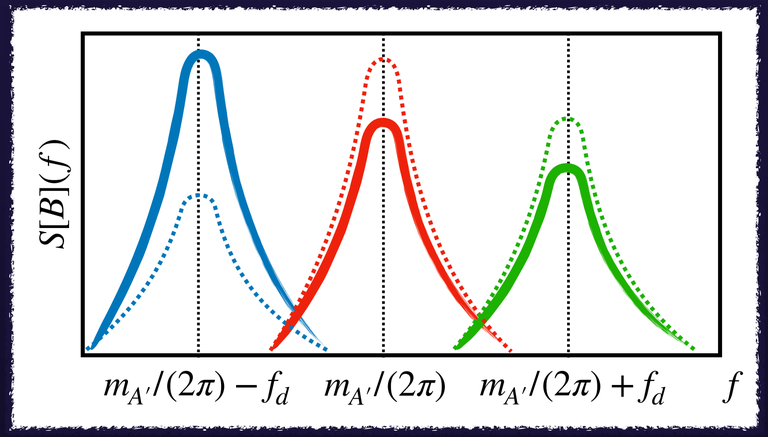

- Signal derivation holds for $10^{-21}\,\text{eV} \lesssim m_{A'} \lesssim 1/R_\oplus \sim 3 \times 10^{-14}\,\text{eV}$

Note: mass range $1/L_{\rm magnetosphere} \sim 10^{-16}\,\text{eV} \lesssim m_{A'} \lesssim 3 \times 10^{-14}\,\text{eV} \sim 1/R_\oplus$ can have large corrections

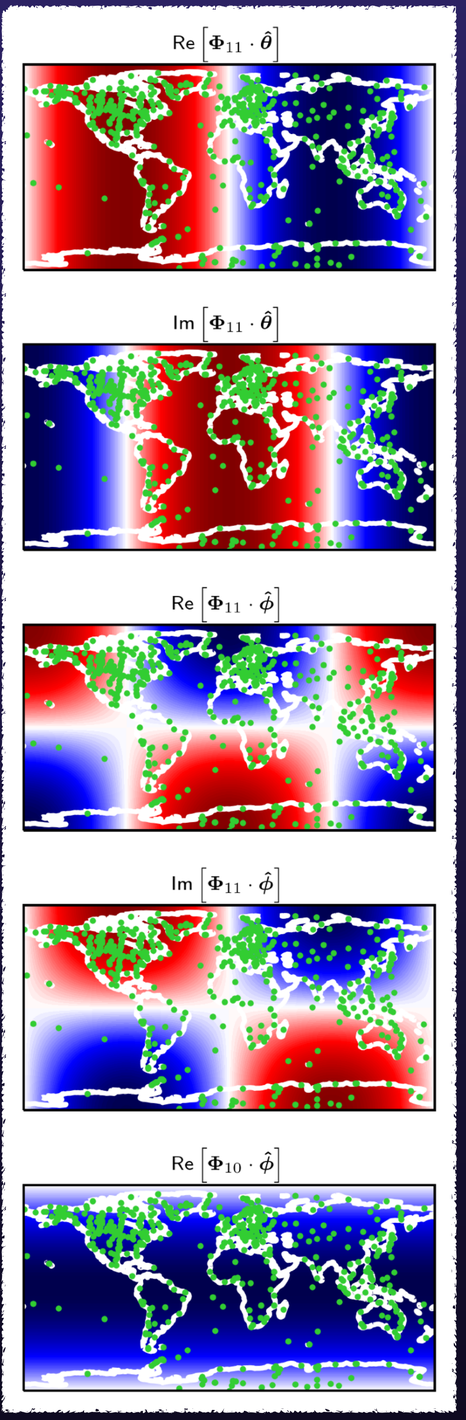

What about the axion?

Rough translation

$$\varepsilon m_{A'} \leftrightarrow g_{\phi\gamma} B_\oplus$$

Assuming DM field-amplitude normalisations

- A similar signal arises, because of the Earth's static geomagnetic field $\mathbf{B}_\oplus$!
- $\mathscr{L} \supset \frac{g_{\phi\gamma}}{4}\phi F\tilde{F} = g_{\phi\gamma}\phi\mathbf{E}\cdot\mathbf{B} \longrightarrow g_{\phi\gamma}(\partial_t\phi)\mathbf{B}_\oplus\cdot\mathbf{A} \sim -ig_{\phi\gamma}m_\phi\phi\mathbf{B}_\oplus\cdot\mathbf{A}$
- Once again, looks like an effective current: $\mathbf{J}_{\rm eff} = ig_{\phi\gamma}m_\phi\phi\mathbf{B}_\oplus$
- $\hat{\mathbf{B}}_\oplus$ plays the role of $\hat{\mathbf{A}}'_I$
- Use the International Geomagnetic Reference Field (IGRF-13) model for $\mathbf{B}_\oplus$

[Earth Planets Space **73** (2021) 49]

Fixed by IGRF-13

$$\mathbf{B}(\tilde{\Omega},t) = -i(g_{\phi\gamma}\phi_0)(m_\phi R_\oplus)\sum_{l,m}\frac{C_{lm}}{l}\tilde{\mathbf{\Phi}}_{lm}(\tilde{\Omega})e^{-im_\phi t}$$

$$B \sim 1\,\mathrm{nG}\times\left(\frac{g_{\phi\gamma}}{10^{-10}\,\mathrm{GeV}^{-1}}\right)$$

where $\frac{1}{2}m_\phi^2\langle\phi_0^2\rangle_{T\gg T_{\rm coh}} = \rho_{\rm DM}$

- Signal still found in one type of VSH, but get higher multipoles l from Earth's field
- Sourcing magnetic field is co-rotating with the ground-based detectors: frequency content now only at $f = m_{A'}/(2\pi)$

$1\,\mathrm{G} = 10^{-4}\,\mathrm{T}$

PRD (in press) [arXiv:2112.09620]

A overview of our analysis (DPDM) I

- Our signal lives in a few VSH: $\mathbf{B}_{\rm signal}(\tilde{\Omega}, t) \propto \sum_{m=-1}^{1} A'_m \tilde{\mathbf{\Phi}}_{1m}(\tilde{\Omega}) e^{-i(m_{A'} - 2\pi f_d m)t}$.
- Per-station projection of data onto the signal: $\mathbf{B}_{\rm signal}(\tilde{\Omega}_i, t_j) \cdot \mathbf{B}^i_{\rm data}(t_j) = \sum_{n=1}^{5} a_i^{(n)} X_i^{(n)}(t_j)$
- The $X_i^{(n)}(t_j) \sim \{\mathrm{Re}, \mathrm{Im}\}[\Phi^{\theta,\phi}_{1,\{1,0\}}(\tilde{\Omega}_i)] \times B^{\theta,\phi}_{\rm data}(t_j)]$ depend on data; the $a_i^{(n)}(t_j)$ capture the expected signal properties.
- Stations turn on and off, have time-variable noise, etc.
- Within each calendar year, we combine all stations inverse-variance weighted by data-driven estimate of white-noise level in stations:

$$X^{(n)}(t_j) = [W^{(n)}(t_j)]^{-1} \sum_{\{i | t_j \in \mathcal{T}_i\}} w_i^{(n)}(t) X_i^{(n)}(t_j)$$

- Idea: FT these time-series; search for excess narrowband power over broadband noise.
- Analysis uses sliding time-duration T for coherent analysis to keep $T \sim T_{\rm coh}(f)$ within 3%. Signal never resolved; avoid dependence on lineshape.
- Available data into K different coherence times; searches stacked incoherently.
- Because of the shifted frequency dependence of $m = \pm 1$ modes of DPDM signal, must keep FT at $f = m_{A'}/(2\pi) + m f_d; \quad m = 0, \pm 1$
- 15-dimensional “analysis vectors” $\overrightarrow{X}_k$ that hold info on FT of $X^{(n)}(t_j)$ for $n = 1,\ldots,5$ for 3 frequencies.

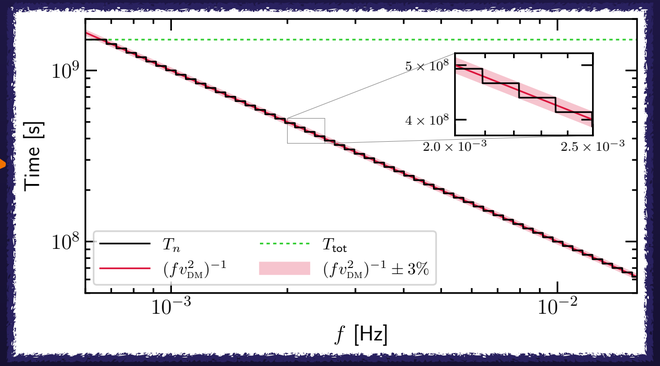

A overview of our analysis (DPDM) II

- Do the same for data = signal: $\langle \vec{X}_k \rangle = \varepsilon \sum_{i=x,y,z} c^*_{ik} \vec{\mu}_{ik}$

SIGNAL SIZE

DPDM POLARIZATION

SIGNAL PATTERN

- Have: data reduction, and signal expectation in that data reduction.
- Need noise!
- Estimated directly from data. Modelling would be extremely hard, unreliable.

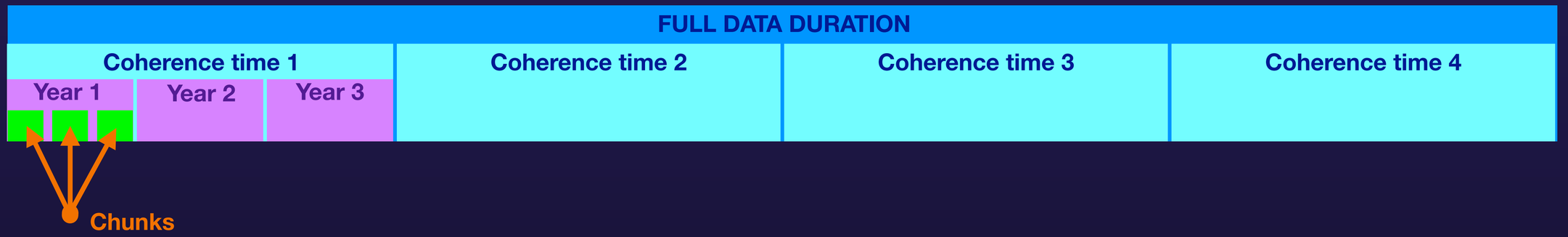

- Use each chunk as an independent noise realisation within a year
- Get PSD of data variation. Average over chunks.
- Procedure yields a data-driven estimate for the noise PSD averaged over broadband frequency ranges.
- Then construct covariance matrix for the analysis vectors $\vec{X}_k$; call this Σ_k
- We validate: (1) Gaussianity of the noise by studying distribution neighbouring frequencies, (2) statistical stationarity of PSDs of the “chunks” (noise realizations) within calendar years, (3) independence of noise estimate on chunk length.

A overview of our analysis (DPDM) III

- Now construct likelihood: $-\ln \mathscr{L}_k\left(\varepsilon, \mathbf{c}_k \middle| \vec{X}_k\right) = \left(\vec{X}_k - \varepsilon \sum_i c_{ik}^* \vec{\mu}_{ik}\right)^\dagger \Sigma_k^{-1} \left(\vec{X}_k - \varepsilon \sum_i c_{ik}^* \vec{\mu}_{ik}\right)$

  NOISE; DATA; SIGNAL SIZE; DPDM POLARIZATION; SIGNAL PATTERN

- Re-write using a projection onto the signal subspace: $-\ln \mathscr{L}_k\left(\varepsilon, \mathbf{d}_k \middle| \mathbf{Z}_k\right) \equiv \left|\mathbf{Z}_k - \varepsilon S_k \mathbf{d}_k\right|^2$

  DATA (NOISE NORMALIZED); SIGNAL SIZE; SIGNAL PATTERN (NOISE NORMALIZED); DPDM POLARIZATION

- Stack coherence times: $\mathscr{L}\left(\varepsilon, \{\mathbf{d}_k\} \middle| \{\mathbf{Z}_k\}\right) \equiv \prod_k \mathscr{L}_k\left(\varepsilon, \mathbf{d}_k \middle| \mathbf{Z}_k\right).$

- But DPDM behaves stochastically over multiple coherence times; the $\mathbf{d}_k$ are drawn from a distribution: $\mathscr{L}_k\left(\mathbf{d}_k\right) = \exp\left(-3\,|\mathbf{d}_k|^2\right)$
- Work in quasi-Bayesian framework and marginalise over $\mathbf{d}_k$ distribution
- Derive posterior on ε (we assume a Jeffrey's prior [Nat. Comm. **12** (2021) 7231])
- Draw limits as 95% credible upper limits from posterior.
- We correct limits for a small (25%) inaccuracy in this approach since signal not strictly exactly monochromatic (discovered by signal injection).

DPDM Results II

PRD **104**, 075023 (2021)
PRD **104**, 095032 (2021)

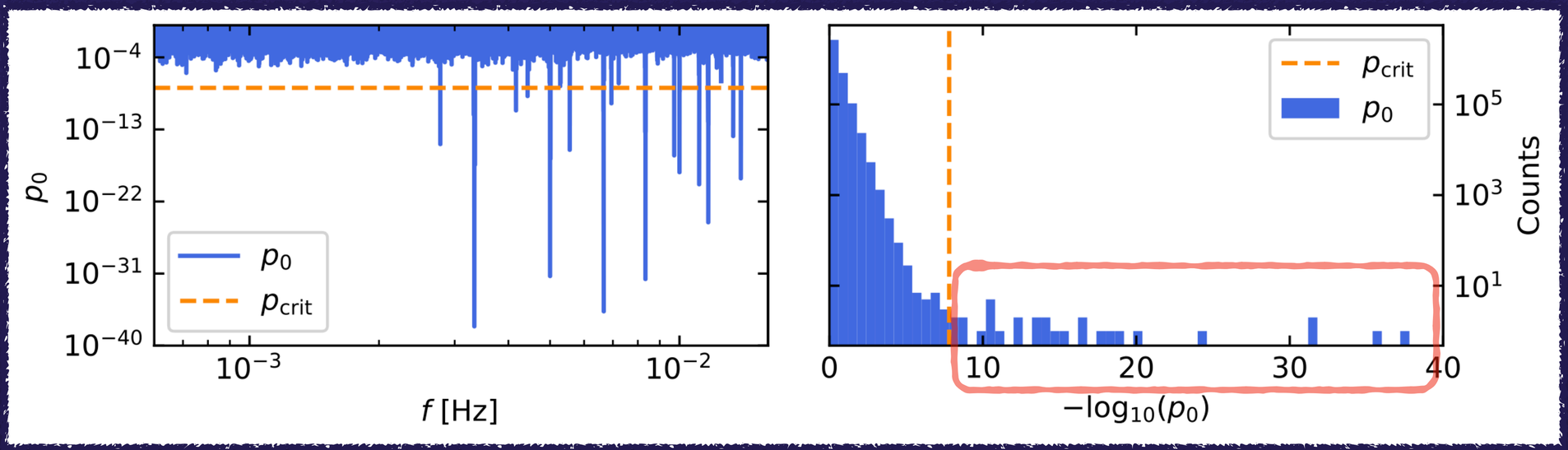

- 30 naive signal candidates identified
- Reject 24 completely on the basis of **robustness tests** for spatial consistency, temporal constancy.
- 6 remaining candidates are in tension with at least one of the checks (or are otherwise problematic); further work might be required to definitively exclude.
- E.g.: candidate at 3.344939mHz has a 6.1σ global significance, but $p = 0.034$ on the temporal constancy robustness check ($p = 0.97$ on the spatial check).
- **We do not claim any robust evidence for a DPDM signal**

PRD **104**, 075023 (2021)
PRD **104**, 095032 (2021)

Validation of injected-signal recovery

- We validated that an injected signal would be recovered by our analysis, with appropriate parameters*

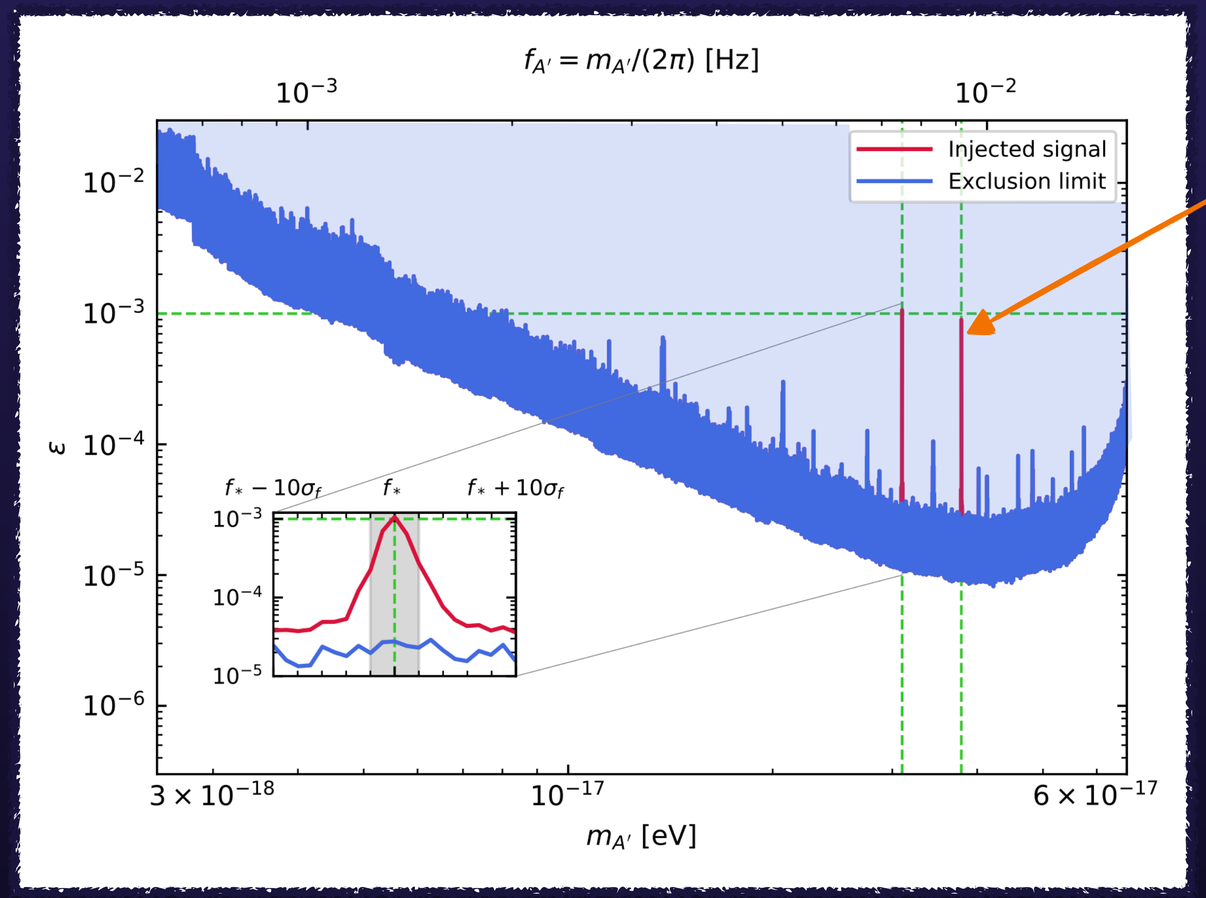

Nyquist reflection of injected signal

*This analysis identified a small (25%) inaccuracy in our original limit-setting procedures, arising from a violation of the assumed exactly monochromatic signal. Size of effect is as expected taking into account a signal with width $1/T_{\mathrm{coh}}$. We degrade to account for this.

Noise Normalization, Gaussianity

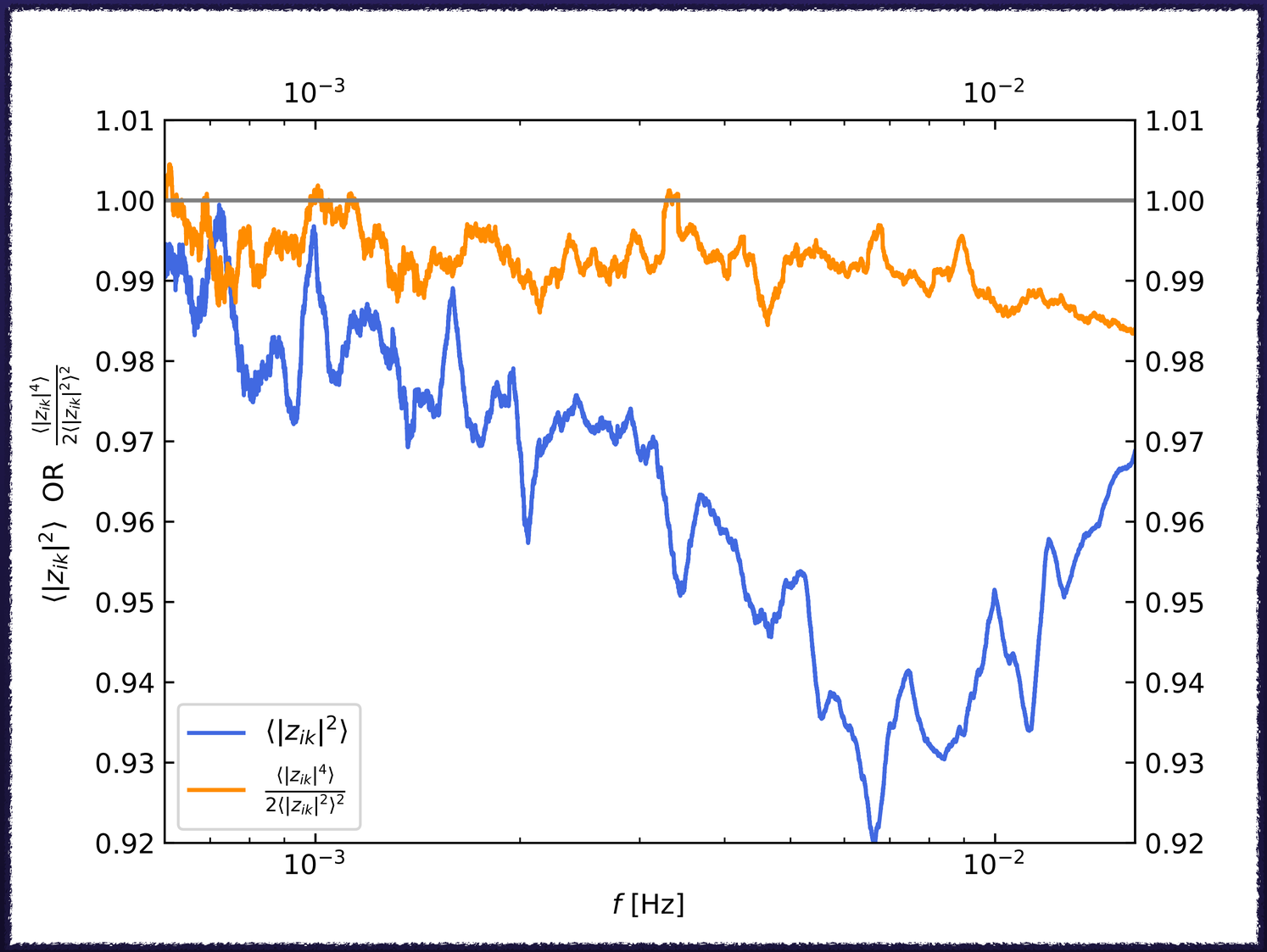

DPDM

Noise Stationarity I - Diagonal elements of Cov. Matrix

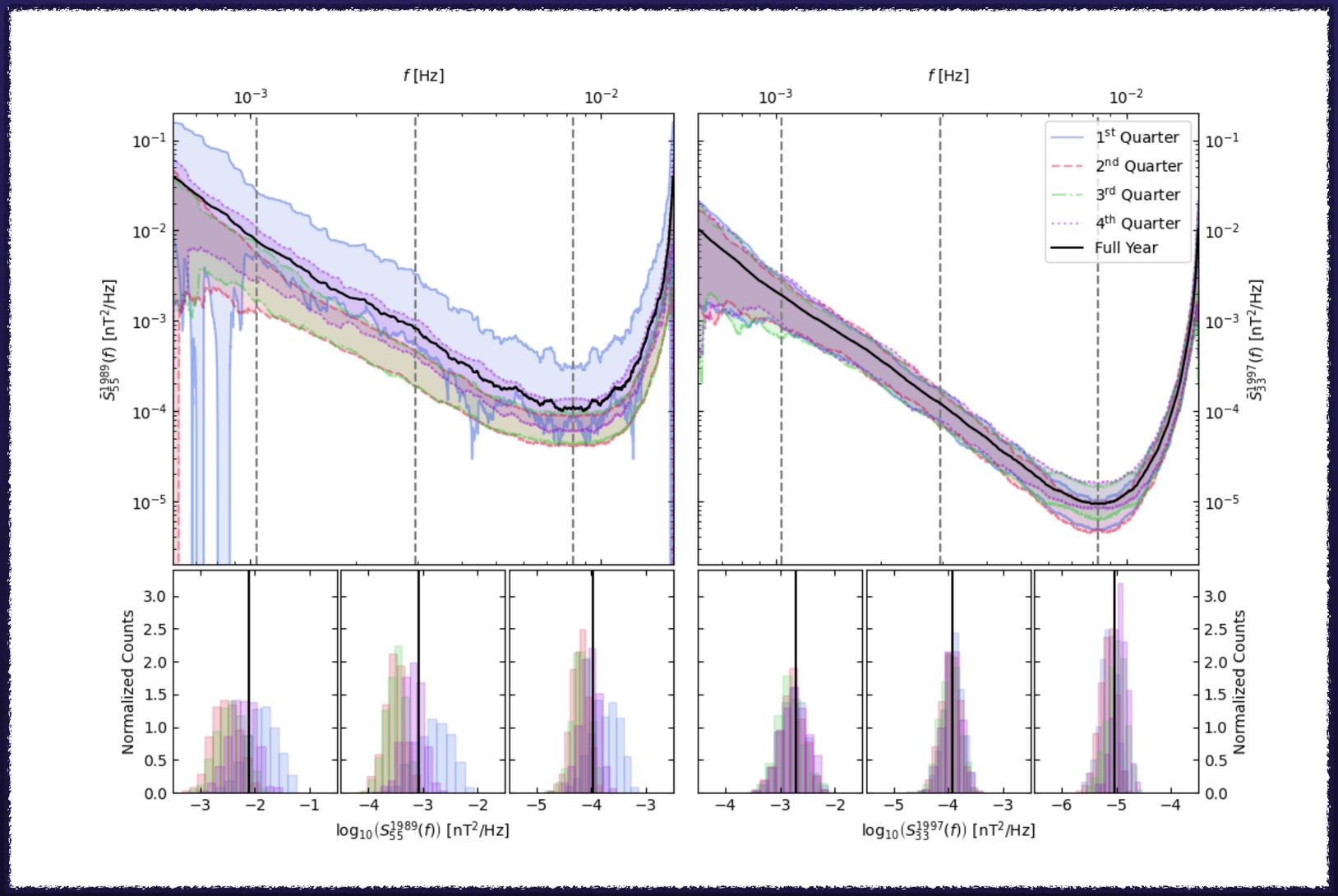

DPDM

Noise Stationarity I - Off-diagonal elements of Cov. Matrix

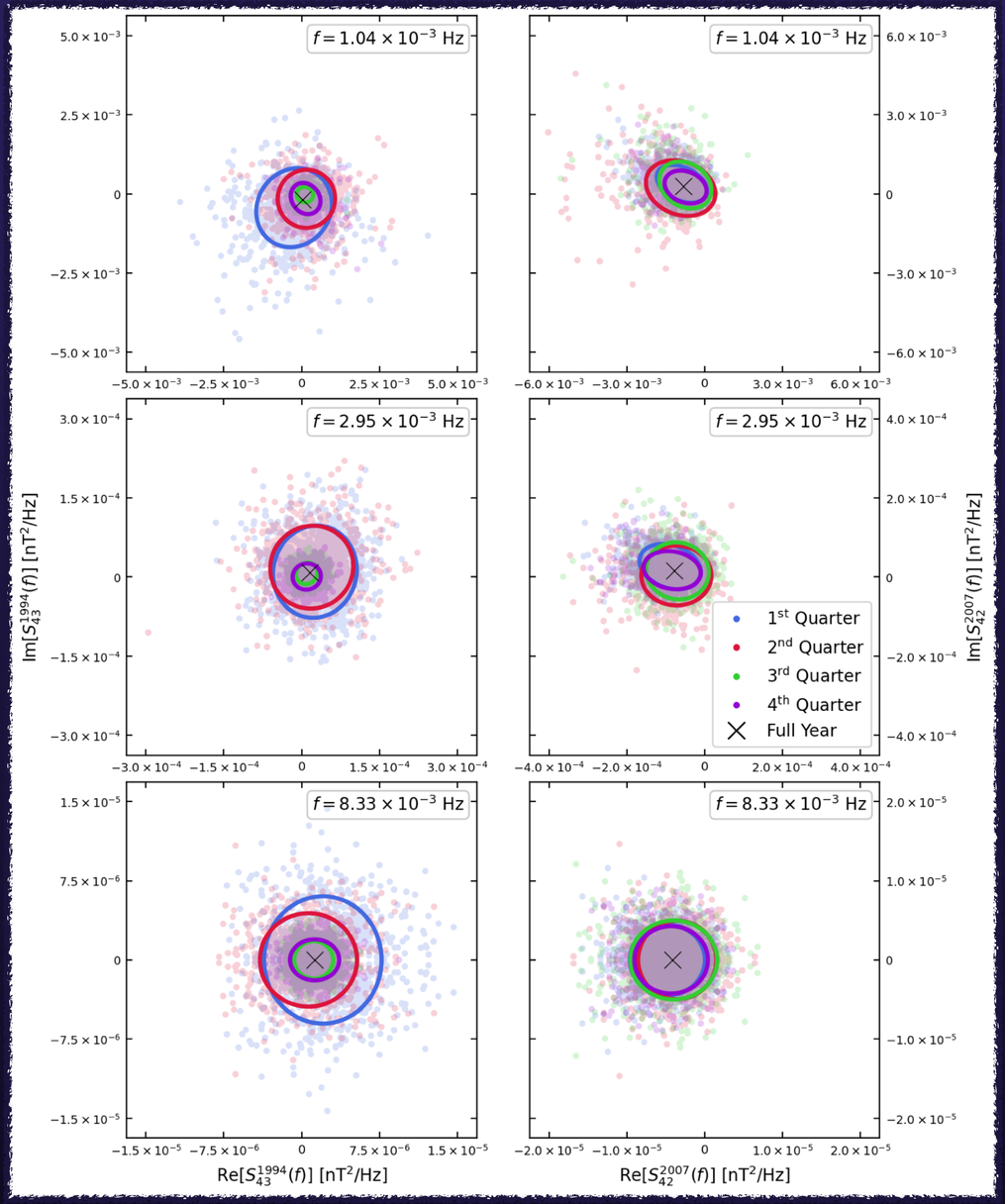

DPDM

Noise Dependence on Chunk Duration

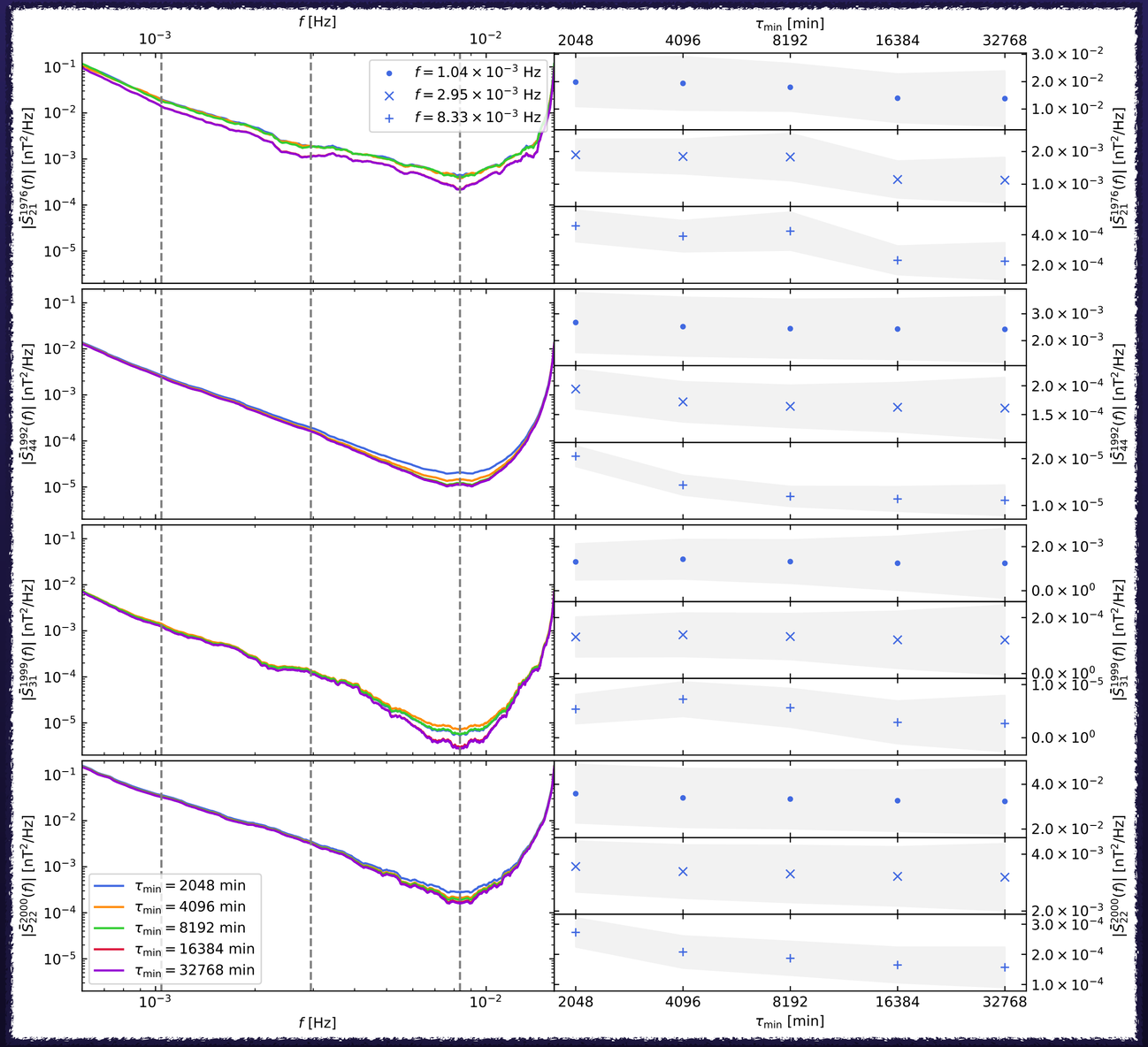

DPDM

DPDM Naive Candidates

Strong tension with temporal + combined tests

Strong tension with temporal test

Strong tension with combined test

Pass all checks, weak, near Nyquist

No.	f [mHz]	p_0	$\sigma(p_0)$	p_1	p_2	p_3	p_4	p_{time}	p_5	p_6	p_7	p_8	p_{geo}	p_{full}
1	2.777776	1.5×10^{-15}	5.7	0.96	0.94	0.10	0.00	7.5×10^{-4}	0.90	0.39	0.12	1.00	9.1×10^{-4}	6.9×10^{-6}
2	2.777779	2.6×10^{-11}	3.8	0.94	0.90	0.21	0.00	0.015	0.99	0.06	0.18	0.99	2.7×10^{-3}	3.2×10^{-4}
3	3.321727	7.0×10^{-12}	4.1	0.97	0.62	0.01	0.01	2.3×10^{-3}	0.59	0.84	0.49	0.18	0.79	0.026
4	3.333330	1.2×10^{-9}	2.7	0.98	0.78	0.11	0.00	3.8×10^{-3}	0.03	0.09	0.01	0.44	0.023	6.7×10^{-4}
5	3.333333	2.6×10^{-38}	11.7	0.97	0.57	0.01	0.00	4.2×10^{-5}	0.07	0.00	0.00	0.79	3.3×10^{-5}	1.9×10^{-8}
6	3.344939	3.9×10^{-18}	6.7	0.99	0.78	0.46	0.01	0.034	0.61	0.51	0.36	0.28	0.97	0.27
7	4.166664	2.4×10^{-11}	3.8	0.39	0.35	0.57	0.05	0.62	1.00	0.01	0.17	0.38	1.1×10^{-3}	9.7×10^{-3}
8	4.432841	1.5×10^{-9}	2.6	1.00	0.84	0.56	0.14	0.051	0.47	0.73	0.81	1.00	0.091	0.023
9	4.999999	4.9×10^{-32}	10.4	0.99	0.71	0.08	0.00	9.0×10^{-5}	0.10	0.12	0.00	0.98	3.6×10^{-3}	3.7×10^{-6}
10	5.011607	2.2×10^{-17}	6.4	0.97	0.83	0.75	0.00	3.1×10^{-3}	0.94	0.41	0.09	0.81	0.25	6.6×10^{-3}
11	5.555552	5.2×10^{-9}	2.1	0.17	0.98	0.27	0.01	0.031	0.25	0.88	0.09	1.00	3.5×10^{-4}	1.1×10^{-4}
12	5.555557	2.9×10^{-16}	6.0	1.00	0.59	0.35	0.00	1.0×10^{-3}	1.00	0.10	0.88	1.00	3.7×10^{-4}	4.0×10^{-6}
13	6.655058	2.0×10^{-11}	3.8	1.00	0.44	0.90	0.49	0.058	0.74	0.96	0.59	0.98	0.11	0.031
14	6.666665	1.9×10^{-36}	11.3	1.00	0.94	0.10	0.00	2.0×10^{-5}	0.99	0.02	0.02	0.86	2.8×10^{-3}	7.1×10^{-7}
15	6.944447	1.8×10^{-10}	3.2	1.00	0.34	0.60	0.03	1.7×10^{-3}	0.98	0.98	0.86	1.00	8.4×10^{-7}	2.3×10^{-8}
16	8.321724	5.2×10^{-14}	5.1	0.98	1.00	0.07	0.11	1.1×10^{-4}	0.88	0.94	1.00	0.94	5.6×10^{-3}	6.6×10^{-6}
17	8.333325	4.5×10^{-11}	3.6	0.82	0.61	0.39	0.03	0.36	0.43	0.54	0.17	0.90	0.67	0.55
18	8.333333	2.1×10^{-32}	10.5	0.99	0.59	0.83	0.00	1.2×10^{-3}	1.00	0.42	0.79	1.00	6.8×10^{-5}	9.5×10^{-7}
19	8.333342	4.5×10^{-11}	3.6	0.82	0.61	0.39	0.03	0.36	0.43	0.54	0.17	0.90	0.67	0.55
20	8.344942	5.2×10^{-14}	5.1	0.98	1.00	0.07	0.11	1.1×10^{-4}	0.88	0.94	1.00	0.94	5.6×10^{-3}	6.6×10^{-6}
21	9.722222	5.7×10^{-17}	6.2	1.00	0.14	0.64	0.00	2.5×10^{-5}	0.99	0.95	0.94	1.00	1.0×10^{-6}	4.1×10^{-10}
22	9.999996	4.6×10^{-19}	7.0	1.00	0.99	0.40	0.03	2.2×10^{-4}	1.00	0.01	0.11	0.44	7.5×10^{-3}	1.7×10^{-5}
23	10.00001	1.3×10^{-14}	5.3	1.00	0.88	0.45	0.16	5.0×10^{-5}	0.64	0.47	0.04	0.95	0.25	2.2×10^{-4}
24	10.01160	5.7×10^{-9}	2.1	0.98	0.47	0.98	0.80	0.062	0.86	0.42	0.95	0.98	0.076	0.023
25	11.11111	1.4×10^{-20}	7.5	1.00	0.36	0.07	0.00	7.5×10^{-6}	1.00	0.39	0.81	1.00	1.2×10^{-4}	1.3×10^{-8}
26	11.65507	9.3×10^{-13}	4.5	1.00	1.00	0.99	0.56	3.7×10^{-7}	1.00	0.61	0.97	1.00	5.4×10^{-7}	3.7×10^{-12}
27	11.66667	2.6×10^{-25}	8.8	1.00	0.89	0.22	0.00	1.1×10^{-4}	0.01	0.19	0.04	1.00	2.0×10^{-3}	2.4×10^{-6}
28	11.67827	3.9×10^{-13}	4.7	0.92	0.99	0.97	0.10	10.0×10^{-3}	0.99	0.88	0.31	0.48	0.12	7.5×10^{-3}
29	13.33334	1.5×10^{-14}	5.3	1.00	0.98	0.71	0.00	3.2×10^{-4}	0.31	0.34	0.43	0.99	0.34	1.5×10^{-3}
30	13.88889	7.8×10^{-20}	7.2	0.98	0.98	0.26	0.00	4.1×10^{-6}	0.67	0.02	0.71	1.00	3.6×10^{-7}	2.5×10^{-11}

Axion Naive Candidates

Strong tension with geographical + combined tests

Strong tension with temporal test

Pass all checks, weak, near Nyquist

No.	f [mHz]	p_0	$\sigma(p_0)$	p_1	p_2	p_3	p_4	p_{time}	p_5	p_6	p_7	p_8	p_{geo}	p_{full}
1	2.777777	6.6×10^{-17}	6.2	0.85	0.81	0.01	0.01	6.4×10^{-3}	1.00	0.90	0.05	0.47	0.025	1.1×10^{-3}
2	3.333331	1.8×10^{-12}	4.4	1.00	0.99	0.58	0.05	8.8×10^{-4}	0.76	1.00	0.37	0.24	4.9×10^{-4}	4.5×10^{-6}
3	3.333335	3.0×10^{-37}	11.5	0.99	0.91	0.30	0.02	0.013	0.43	1.00	0.23	0.10	1.1×10^{-3}	1.3×10^{-4}
4	3.333338	1.2×10^{-10}	3.4	0.96	0.93	0.05	0.03	0.011	0.08	0.99	0.00	0.10	2.0×10^{-4}	2.2×10^{-5}
5	4.166668	3.5×10^{-18}	6.7	0.91	0.35	0.29	0.01	0.14	1.00	0.58	0.04	0.37	0.033	0.023
6	5.000000	9.8×10^{-62}	15.6	0.64	0.84	0.35	0.00	0.022	0.01	1.00	0.48	0.02	8.0×10^{-6}	2.7×10^{-6}
7	5.532406	4.5×10^{-11}	3.6	1.00	0.08	0.07	0.32	0.016	0.46	0.54	0.89	0.20	0.74	0.091
8	5.555552	5.1×10^{-9}	2.1	0.62	0.95	0.49	0.48	0.74	1.00	0.96	0.05	0.63	4.3×10^{-7}	2.5×10^{-5}
9	5.555557	6.0×10^{-12}	4.1	0.97	0.41	0.49	0.45	0.58	1.00	0.77	0.55	1.00	2.8×10^{-6}	6.9×10^{-5}
10	6.666661	9.8×10^{-17}	6.2	0.99	0.83	0.11	0.07	0.027	0.13	1.00	0.78	0.51	3.1×10^{-7}	1.8×10^{-7}
11	6.666668	1.7×10^{-78}	17.9	0.19	0.96	0.34	0.04	0.12	0.63	1.00	0.31	0.08	6.3×10^{-11}	5.5×10^{-10}
12	6.944444	2.2×10^{-15}	5.7	1.00	0.75	0.45	0.01	8.5×10^{-3}	1.00	0.97	0.26	0.96	4.7×10^{-6}	6.0×10^{-7}
13	6.944451	1.3×10^{-9}	2.6	0.31	0.97	0.46	0.01	0.051	1.00	0.77	0.49	0.77	0.034	9.8×10^{-3}
14	7.777782	2.0×10^{-9}	2.5	1.00	0.85	0.01	0.27	3.7×10^{-3}	0.80	0.72	0.39	0.99	0.16	4.5×10^{-3}
15	8.310182	3.4×10^{-9}	2.3	0.81	0.14	0.02	0.76	0.14	0.81	0.25	0.12	0.98	0.11	0.068
16	8.333333	2.9×10^{-41}	12.2	0.98	0.00	0.36	0.06	7.8×10^{-3}	0.98	1.00	0.64	0.82	5.5×10^{-6}	6.4×10^{-7}
17	8.356485	3.4×10^{-9}	2.3	0.81	0.14	0.02	0.76	0.14	0.81	0.25	0.12	0.98	0.11	0.068
18	8.888885	4.7×10^{-12}	4.2	1.00	0.78	0.07	0.36	7.9×10^{-3}	0.86	0.88	0.68	1.00	0.045	2.4×10^{-3}
19	9.722221	1.6×10^{-19}	7.1	0.95	0.96	0.29	0.00	1.5×10^{-3}	1.00	1.00	0.36	0.99	3.7×10^{-13}	2.5×10^{-14}
20	10.00000	5.2×10^{-87}	19.0	0.98	0.88	0.22	0.01	0.012	0.70	1.00	0.09	0.05	1.3×10^{-11}	7.2×10^{-12}
21	11.08796	7.2×10^{-9}	2.0	1.00	0.09	0.91	0.15	2.8×10^{-7}	0.68	0.98	1.00	0.97	1.5×10^{-5}	7.5×10^{-11}
22	11.11111	4.6×10^{-16}	5.9	0.99	0.95	0.77	0.02	7.8×10^{-3}	1.00	0.97	0.32	1.00	1.6×10^{-13}	7.4×10^{-14}
23	11.38889	8.5×10^{-9}	1.9	1.00	0.81	0.46	0.09	2.6×10^{-3}	0.99	0.30	0.82	0.96	0.042	8.6×10^{-4}
24	11.66666	3.7×10^{-56}	14.8	0.83	0.97	0.41	0.00	1.8×10^{-4}	0.05	1.00	0.38	0.05	2.0×10^{-14}	1.6×10^{-16}
25	12.50000	3.9×10^{-23}	8.2	1.00	0.84	0.80	0.00	4.5×10^{-4}	1.00	1.00	0.13	0.44	5.2×10^{-10}	6.1×10^{-12}
26	13.33333	1.1×10^{-49}	13.7	0.98	0.96	0.13	0.00	8.2×10^{-7}	0.00	1.00	0.00	0.02	1.6×10^{-14}	4.6×10^{-19}
27	13.88889	9.0×10^{-25}	8.6	0.75	0.97	0.02	0.00	6.9×10^{-4}	1.00	1.00	0.00	0.08	2.2×10^{-7}	2.7×10^{-9}